NASA Technical Paper 1094

Influence of Oil-Squeeze-Film Damping on Steady-State Response of Flexible Rotor Operating to Supercritical Speeds

Robert E. Cunningham

DECEMBER 1977

NASA

NASA Technical Paper 1094

Influence of Oil-Squeeze-Film Damping on Steady-State Response of Flexible Rotor Operating to Supercritical Speeds

Robert E. Cunningham
Lewis Research Center
Cleveland, Ohio

INFLUENCE OF OIL-SQUEEZE-FILM DAMPING ON STEADY-STATE RESPONSE

OF FLEXIBLE ROTOR OPERATING TO SUPERCRITICAL SPEEDS

by Robert E. Cunningham

Lewis Research Center

SUMMARY

The response of a long, slender, ball-bearing-supported rotor was measured for unbalances ranging from 0.62 to 15.1 gram-centimeters. Three unbalance distributions were also evaluated. The test apparatus contained squeeze-film dampers at the bearings, and the rotor could be operated with or without the dampers being activated. Results of undamped and damped responses were compared with an unbalance response computer program by using a mathematical model which closely simulated the actual hardware.

Squeeze-film damping coefficients were calculated from measured data and compared with theoretical short-journal-bearing approximations over a frequency range from 5000 to 31 000 cycles per minute. The dampers were fed at the center from a circumferential oil distribution groove and had a length-diameter ratio of 0.094.

Experimental damping coefficients were in good agreement with values calculated from short-journal-bearing theory. The values generally remained constant over the frequency range investigated.

Squeeze-film dampers located at the bearings were very effective in reducing amplitudes of motion at the rotor ends. As much as 88 percent reduction in amplitude was achieved at resonance for a total unbalance of 0.93 gram-centimeter distributed in a line and in the same phase over three disks.

When oil-squeeze-film dampers were activated for an in-line, alternating-phase unbalance distribution, three distinct resonant amplitudes were reduced to only one. The mode shape for this one corresponded to the third bending critical.

The oil-squeeze-film dampers were also effective in reducing the amplitudes of motion for nonsynchronous as well as synchronous whirl.

An unbalance response computer program was quite accurate in predicting the response of the experimental rotor having an in-line, in-phase unbalance distribution over the three disks.

Operating the rotor at large eccentricities induced a damper instability characterized by a sudden increase in the eccentricity ratio. This phenomenon has been observed by other investigators and is referred to in the literature as bistable operation.

INTRODUCTION

Continuing efforts to improve the performance of aircraft turbojet engines are resulting in higher and higher operating speeds. Such applications as small helicopters, remotely piloted vehicles (RPV's) and small private and commercial aircraft are calling for increased specific-thrust ratios by reducing the overall weight of powerplants (refs. 1 and 2). Aircraft engine manufacturers are also looking at ways of reducing the power losses in an engine. One obvious loss is the leakage of air between compressor stages. Such losses could be reduced by decreasing the seal clearances, particularly those at compressor blade tips.

Higher rotor operating speeds, lighter powerplant structures, and smaller blade tip clearances will call for greater emphasis on the dynamics of rotors and their bearings and on the manner in which the bearings are mounted in the frame. The combination of lighter rotors and higher operating speeds can result in operation above one or more lateral bending critical speeds. Vibration amplitudes at these critical frequencies can be quite high. The reduction of these vibration amplitudes to an acceptable level will dictate the use of more sophisticated balancing methods. One method currently receiving a great amount of attention is the high-speed, multiplane balancing method described in reference 3.

Sometimes, however, it is not possible to achieve low levels of vibration by balancing alone, particularly with lightly damped ball bearings and the built-up rotor assemblies which compose the modern turbojet engine. These rotors, though balanced well initially, degrade with continued service time. Compressor and fan blades can be damaged by debris ingested at the intake. Loosening of tie bolts in built-up rotor assemblies can change the stiffness of the rotor. Normal wear of rotating components also contributes to a gradual degradation in the balance of the rotors. Thus, techniques other than balancing need to be employed to control both steady-state and transient vibration amplitudes.

Coulomb (dry friction) and viscous-oil shear mechanical dampers have been used for many years to control vibration amplitudes. Normally they have been used in controlling torsional vibrations in all types of rotating machinery (ref. 4). The inherent damping properties of hydrodynamic oil-lubricated bearings were investigated by Hagg and Sankey in 1956 (ref. 5).

It is a well known fact that ball and roller bearings contain very little inherent damping, and such bearings are used almost exclusively in aircraft turbine engines. The availability of lubricating oils and the requirement of large amounts of energy dissipation in a limited space were natural inducements to the ultimate development and use of oil-squeeze-film dampers (ref. 6).

To properly design such a damper, the machinery design engineer must know something about the dynamic characteristics of the rotating system. Normally he has a

2

number of computer programs available to him. Such programs can provide him with the flexible critical speeds and mode shapes of a particular rotor model in graphical output (e.g., ref. 7). The computer program of reference 7 will also draw, to scale, a cross section of the rotor under study and will plot critical speeds as a function of support stiffness. Also available are unbalance response computer programs that can predict the response of almost any type of rotor on flexible, damped supports. Damping coefficients can be an input to the program either as constants or as polynomial functions of rotor speed (ref. 8). The output of such programs, however, is only as accurate as the values of input (e.g., support stiffness and damping characteristics).

A number of analytical papers have been written which develop the equations for calculating squeeze-film damping and stiffness coefficient; two such papers using the short-bearing approximation are references 9 and 10. One of the objectives of this investigation was to determine experimentally damping coefficients for an oil-squeeze-film damper and to compare them with theory.

A second objective of this investigation was to examine the experimental response of a three-disk flexible rotor to varying amounts of unbalance with and without squeeze-film damping at the bearing supports. The results would be compared with an unbalance-response computer program similar to the one described in reference 8. This program, however, was modified to consider only circular orbits, and an iterative solution was added that includes support damping as a function of journal eccentricity ratio.

Unbalances tested varied from a low of 0.62 gram-centimeter to a high of 15.1 gram-centimeters. Three different types of unbalance distributions were investigated:

(1) Type I. Identical set screws were placed in the same radial plane in each of the three rotor disks. The set screw in the center disk, however, was out of phase by 180°.

(2) Type II. Identical set screws were placed in the same radial plane in each of the two end disks only. The two set screws were 180° out of phase.

(3) Type III. Identical set screws were placed in the same radial plane in all three disks. Results were obtained for a rotor speed range from 5000 to 31 000 rpm.

APPARATUS

Mechanical Features

Experimental data were obtained with the apparatus shown in figures 1 to 5. The apparatus consists of a long slender shaft supported in ball bearings which are 48.3 centimeters apart. A single, integral disk is located at midspan, while removable disks of identical size, one at each end (disks 1 and 3 in fig. 2), are located outside the bearings. The rotor is 69.09 centimeters long and has a uniform diameter of 2.54 centimeters between bearings. The disks are 9.5 centimeters in diameter and contain threaded holes
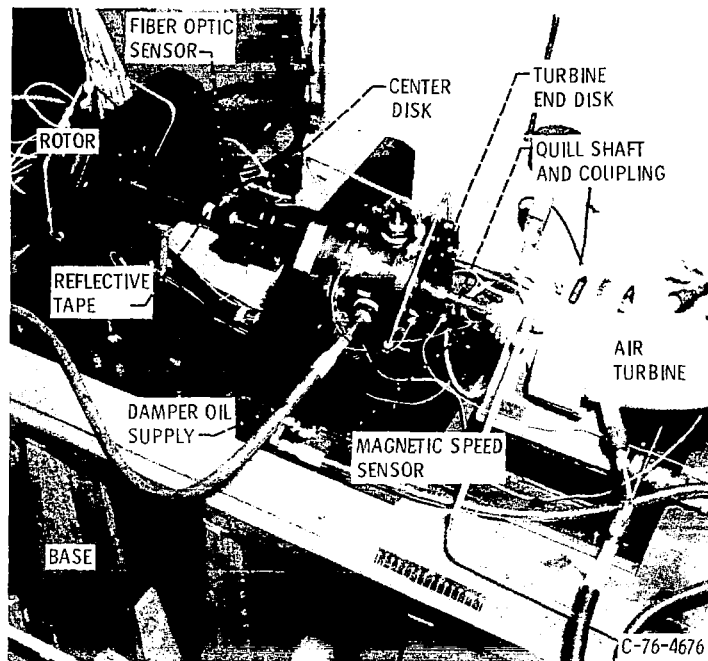
Figure 1. - Test apparatus used in experiments on steady-state unbalance response.

every 10° on a ball circle of 8.26 centimeters. Set screws can be placed in the holes as correction weights for balancing the rotor or to deliberately unbalance the rotor in a particular bending mode.

It was anticipated that severe bending strains would be induced in the rotor, and therefore it is made of a high-strength alloy steel, AISI 4340, which has a minimum yield stress of 1585 meganewtons per square meter.

The rotor is supported in ball bearings, one of which is shown in figure 4. The outer races of these bearings are located in cylindrical steel housings, which also serve as damper journals (figs. 3 and 4). Also shown in figures 3 and 4 are the aluminum centering springs. They provide flexibility in the bearing support, prevent rotation of the damper journal, and center the journal in the damper bearing. The aluminum used for these springs is 6061-T6, which has a yield stress of 296 meganewtons per square meter.

In order to determine the lateral stiffness, the springs were installed in the test rig with the dampers attached and then subjected to known loads in two planes. Deflections were measured and stiffness was calculated from the load, deflection curves. Slopes of these curves were linear, and the average value of the stiffness was 2.36 meganewtons per meter. Values of stiffness in each of the two planes differed by only one-half of 1 percent.

The damper used in this investigation is similar in design to the one described in reference 11, with the following exceptions: No piston ring seals were used at the damper ends, although the grooves were retained (see fig. 3). The piston ring seals
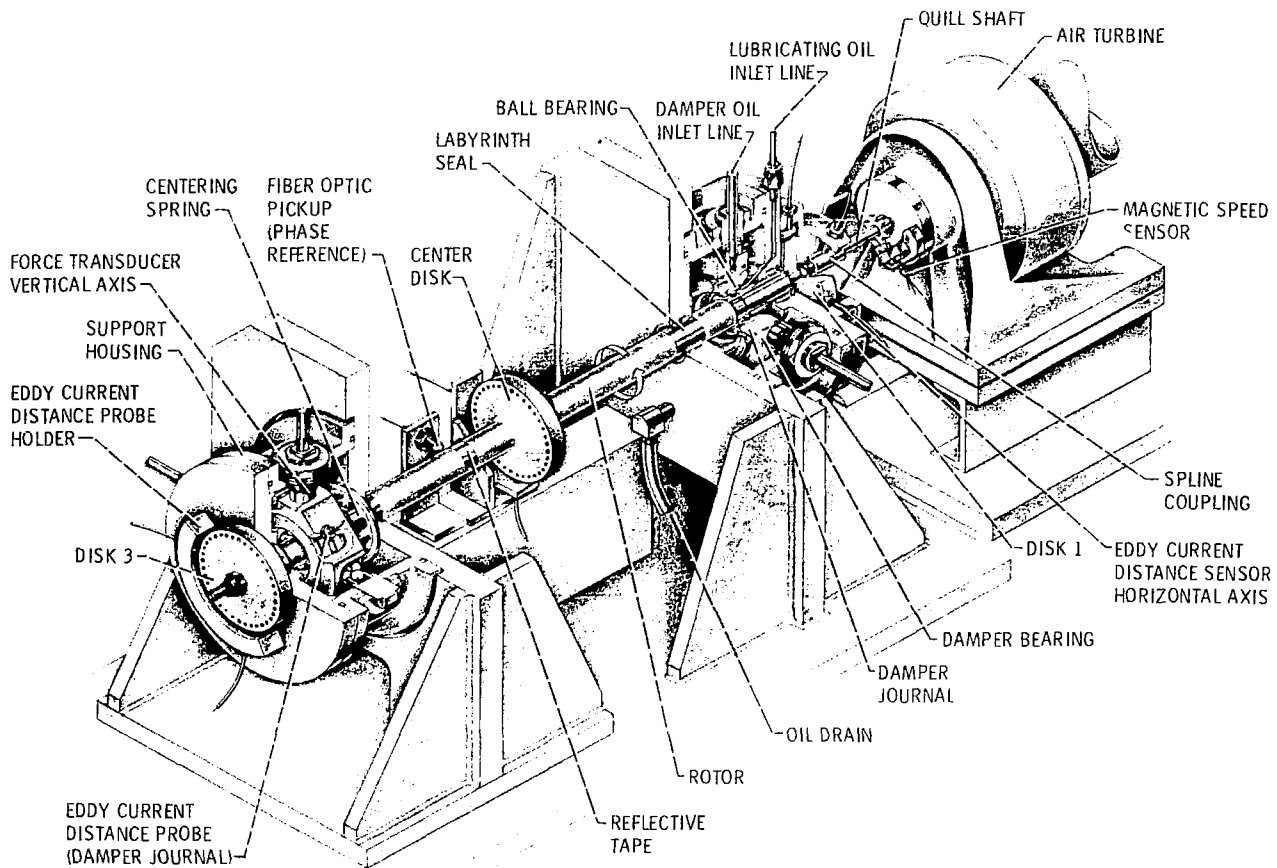
4

Figure 2. - Schematic of test apparatus used in experiments on steady-state unbalance response.

were eliminated because they introduced a tare damping and stiffness that could not be readily quantified. Eliminating the end seals, however, necessitated a reduction in damper radial clearance from 127 micrometers to a nominal clearance of 64 micrometers in order to keep damper oil flows within the pumping capacity of the oil supply system.

The radial, deep-groove ball bearings are 204 series bearings, having a 20-millimeter bore. They are designated high-speed turbine bearings of aircraft quality and have lightweight phenolic retainers. The outer race fits slightly loosely in its housing, and a preload is applied with wave washers. Air-oil mist lubrication for the ball bearings is supplied through three nozzles. The lubricant is a typical turbojet engine oil, type II ester, meeting the specification MIL-L-23699A. The same oil is used in the squeeze-film dampers.

The journals for the squeeze-film dampers are AISI 440-C steel hardened to Rockwell C 58 to 62. The journal outside diameter is 7.9 centimeters, and the width of
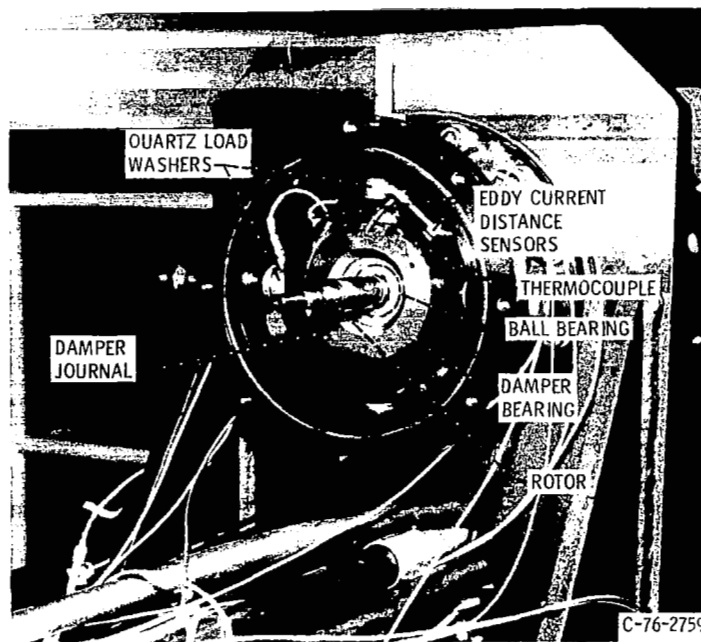
5

R, DAMPER JOURNAL RADIUS, 3.96 cm
L, DAMPER JOURNAL LAND LENGTH, 0.74 cm
C_R, DAMPER RADIAL CLEARANCE, 63.5 μm

Figure 3. - Schematic of oil-squeeze-film damper used in experiments for steady-state response of three-disk rotor.

Figure 4. - Components of flexible damped support.

each of the two lands is 0.74 centimeter, so that the length-diameter ratio is 0.094. Oil is supplied to the two halves of the damper by a circumferential groove 0.64 centimeter wide. The journal outer surface has a 0.2-micrometer finish. The average assembled radial clearance in the dampers is 63.5 micrometers.

The outer damper bearing is held stationary (figs. 2 and 3). It is made of SAE 4340 steel hardened to Rockwell C 45 to 50 and has a 0.2-micrometer finish. The flow of oil to each damper can be controlled independently with needle valves located in each of the supply lines. Temperature of the oil can be maintained within 2^O C over the elapsed time

Figure 5. – End view of test apparatus showing ball bearing 2 and oil-squeeze-film damper.

of a typical test run.

The test rotor is driven by a 10-centimeter-diameter air turbine having a maximum operating speed of 60 000 rpm. The turbine is connected to the test rotor by a 0.95-centimeter-diameter quill shaft and a spline coupling.

Instrumentation

Deflections of the test rotor from a neutral axis were sensed by noncontacting, eddy-current probes. These probes, along with signal conditioners and power supplies, produced a voltage linearly proportional to distance. The approximate linear range for the probes used in this investigation was 900 micrometers. Before any of the eddy-current distance sensors were installed in the test apparatus, each was calibrated with a microm-eter fixture, and voltage output was read on a digital voltmeter. The calibrating fixture was designed by the probe manufacturer specifically for this purpose. A dynamic cal-ibration of several of the probes was made at one distance setting. The same calibrating fixture had a flat plate that could be rotated with a preset wobble underneath the probe be-ing calibrated. The output voltage was recorded and compared with the static calibration; agreement in all cases was good.

7

Figure 6. - Schematic of oil-squeeze-film damper.

Sensors for monitoring shaft motions were located in mutually perpendicular axes at each of the three disks. Distance sensor pairs were also cemented into the damper bearing flush with its surface (figs. 2 and 6). These sensor pairs were displaced 45° from the damper force transducers. The force transducers, located in mutually perpendicular planes, can be seen in figure 5.

The transducers used for measuring the forces transmitted through the damper oil squeeze film are quartz crystal, piezoelectric load washers. The load range is 0 to 35.6×10^3 newtons with a stiffness of 175×10^8 newtons per meter and a resonant frequency of 50 000 hertz. Linearity over the load range was 1 percent.

A fiber optic sensor was used to establish a reference signal for the measurement of phase angles. A piece of reflective tape was epoxied to the rotor surface with one edge coincident with the centerline of one of the balancing holes in the center disk (figs. 1 and 2). The tape was 1.3 centimeters wide and covered exactly 180° of the rotor surface. The square-wave voltage signal produced when the shaft was rotated was used as the reference signal to which other sensor outputs were compared.

A magnetic sensor near a six-toothed wheel mounted on the turbine quill shaft measured rotational frequency (fig. 2). Ball-bearing temperatures were measured with iron-constantan thermocouples and recorded on a strip chart. Damper-oil-film temperatures were monitored on a digital readout. Oil flow rates to the squeeze-film dampers were

8

measured by turbine vane flowmeters located in the supply lines and were read out as frequency on a digital counter.

Leads from the numerous sensors located on the test apparatus were connected to a patch board in the control room. From this board leads were paralleled to any number of readout and data acquisition systems.

For example, the output signals from any one of the displacement or force transducers could be directed into either of two channels of a tracking filter. The filtered output signal, a true sine wave at the rotor frequency, was paralleled to one input terminal of a phase meter and then to a peak-to-peak measuring voltmeter. In the phase meter it was compared with the square waveform generated by the fiber optic sensor. A phase angle was then detected and displayed digitally on a meter and also fed to the Y' axis of an X-Y-Y' plotter. The peak-to-peak voltage, representing either amplitude of motion or transmitted force, was displayed on a meter while simultaneously being recorded on the Y axis of the plotter. Unfiltered signals could also be monitored with any of the readout instruments. Four X-Y curve tracing oscilloscopes were used to monitor simultaneously any of the coordinate axis displacements or transmitted forces.

DISCUSSION OF RESULTS

The results of this investigation are presented in figures 7 to 16 and in table I, and are discussed in two sections. The first examines the response of a three-disk rotor to various magnitudes of unbalance. Three types of unbalance distribution were tested, and results are shown in table I. The second section of the discussion compares experimentally determined damping coefficients with those predicted by theory for unbalances ranging from 0.62 to 15.1 gram-centimeters and rotor frequencies up to 31 000 cycles per minute. These results are plotted in figures 13 to 16.
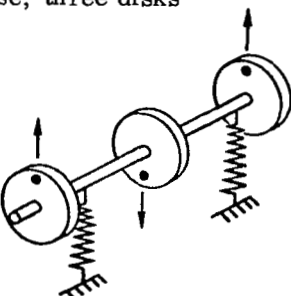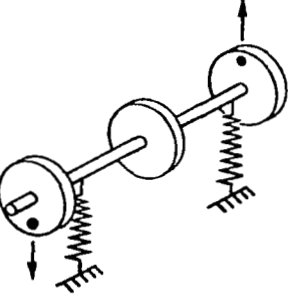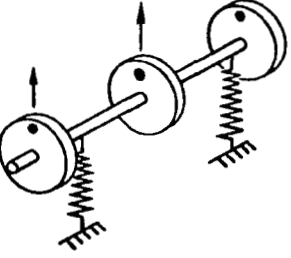
Unbalance Response

Before any tests were conducted, it was necessary to determine the undamped critical speeds and mode shapes. These were determined from the computer program of reference 7 and are plotted in figure 7 for a spring stiffness of 2.36 meganewtons per meter. The deflections were only relative but indicated that oil-squeeze dampers placed at the supports should be effective when operating through all four bending critical speeds.

Before any deliberate unbalance distributions could be tried, the rotor had to be well balanced. First attempts to balance the rotor without any squeeze-film damping at the supports indicated a high degree of sensitivity of a ball-bearing-supported rotor to very

TABLE I. – SUMMARY OF EXPERIMENTAL AND THEORETICAL DAMPING COEFFICIENTS

AT VARYING TYPES AND MAGNITUDES OF UNBALANCE

[Damper geometry shown in fig. 3; type of oil, type II ester meeting specification MIL-L-23699-A; viscosity at 38° C, 0.033 (N)(sec)/m^2; oil flow, 5.15×10^{-4} m^3/min; supply pressure, 0.19 MPa.]

Type of unbalance distribution	Magnitude of total unbalance, U, g-cm	Frequency range, cpm	Average damping coefficient, $B_{\eta=0}$, (N)(sec)/m	
			Experimental	Theoretical
Type I – In-line, alternating-phase, three disks	0.93	11 000 – 31 000	6740	6492
	1.67	10 000 – 31 000	6531	6213
Type II – In-line, alternating-phase, two end disks	0.62	7 000 – 26 000	6029	6213
	1.11	7 000 – 28 000	6265	5408
	1.5	7 000 – 28 000	6843	6212
	3.3	6 000 – 29 000	5416	5880
Type III – In-line, same-phase, three disks	0.93	6 000 – 22 000	5478	5758
	1.67	7 000 – 24 000	5708	5425
	2.25	6 000 – 23 000	5926	5425
	4.97	5 000 – 22 000	5880	5425
	10.6	6 000 – 30 000	5289	6108
	15.1	5 000 – 25 000	6375	6843
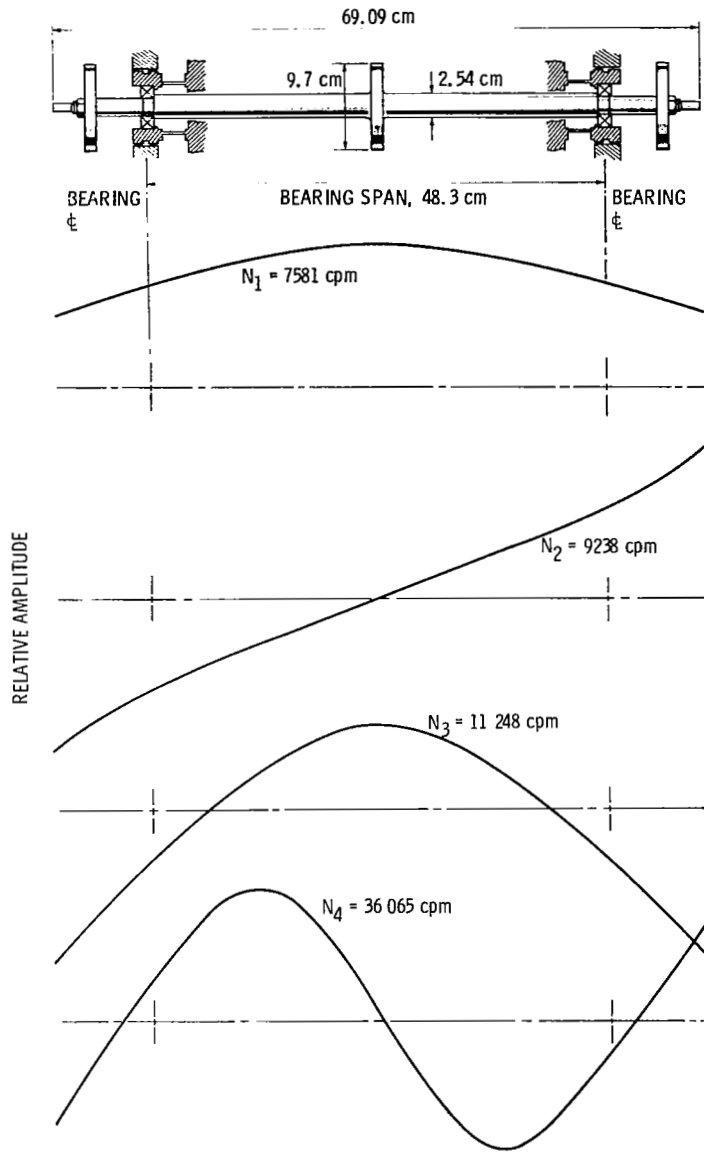
Figure 7. - Undamped critical speeds and mode shapes. Centering spring stiffness, K, 23.63x10^5 newtons per meter.

small amounts of unbalance. Fairly good balance, however, was achieved by using a combination of the influence coefficient method (ref. 3) and single plane balancing. The results of rotor balancing, presented in figure 8, show that peak-to-peak amplitudes of motion at resonance did not exceed 25 micrometers at any of the three disks. A certain amount of machining runout and/or bend was present in the rotor, as shown by this plot. However, it was not possible to reduce this kind of runout further.
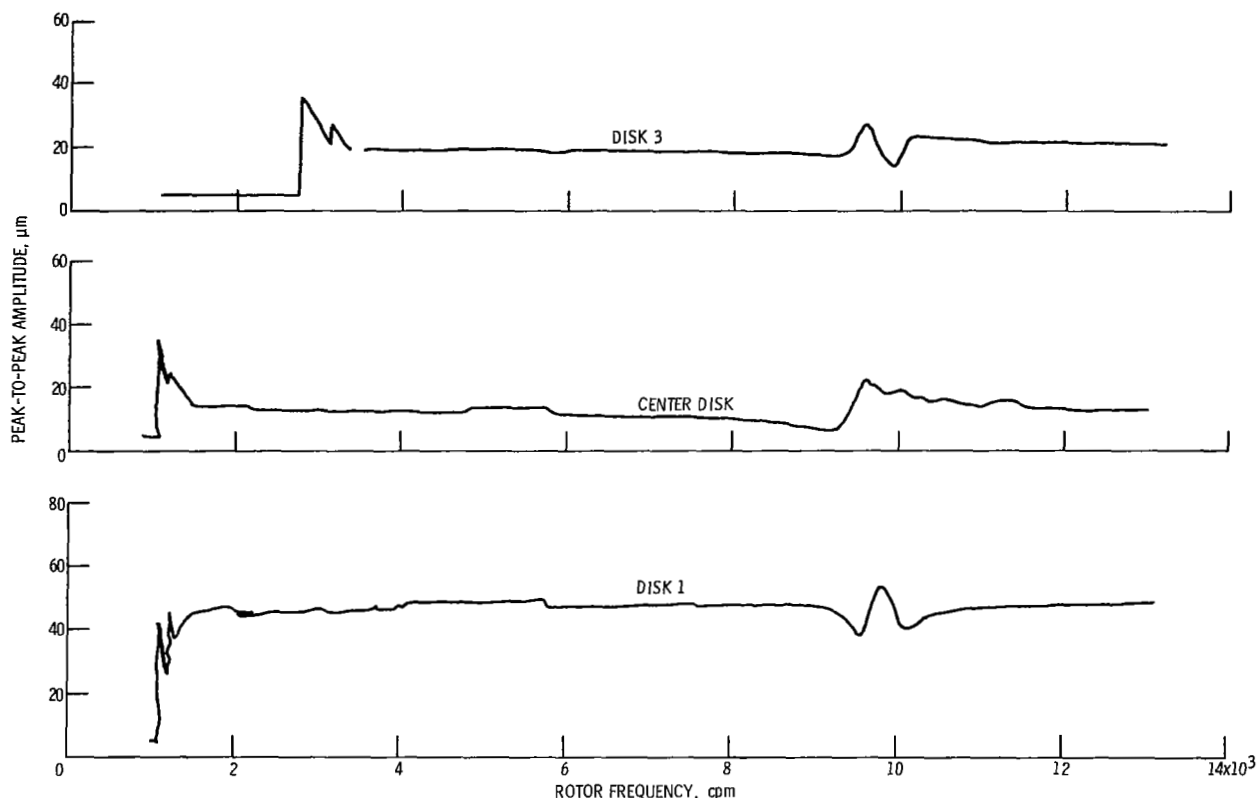
Figure 8. – Final balance of three-disk rotor. Oil dampers activated.

Figures 9 to 13 compare the undamped rotor response with the response when oil-squeeze-film dampers were activated. The traces in figures 9 to 12 are for the filtered signal generated by either proximity distance sensors or piezoelectric crystal force transducers. The 10- and 20-hertz-bandwidth filters track on the rotor frequency, and, therefore, the trace plotted is that of the rotor synchronous response only. Comparisons between undamped and damped response are for rather small unbalances of 0.62 and 0.93 gram-centimeter because operating the rotor without any external damping at the bearings could have resulted in damaging the rotor and stationary seals if larger unbalances had been used.

The plots of amplitude against frequency in figure 9 were produced by an in-line, alternating-phase distribution of weights in the three disks. The unbalance weights in the end disks were placed 180° out of phase with the weight in the center disk, as depicted by the inset drawing. The total unbalance was 0.93 gram-centimeter. The three set screws used as unbalance weights were carefully matched in weight and did not vary more than 4 milligrams.

The amplitudes of motion plotted in figure 9(a) are those of the center disk. A maximum peak-to-peak amplitude of approximately 230 micrometers was recorded for the rotor operating with no externally applied damping.
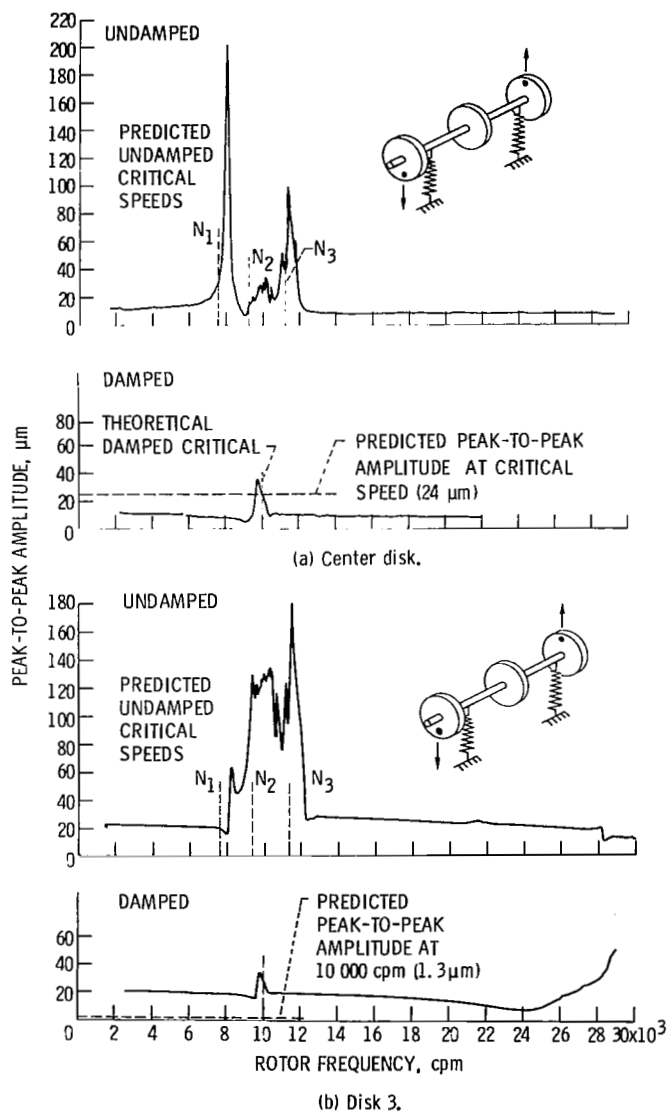
12
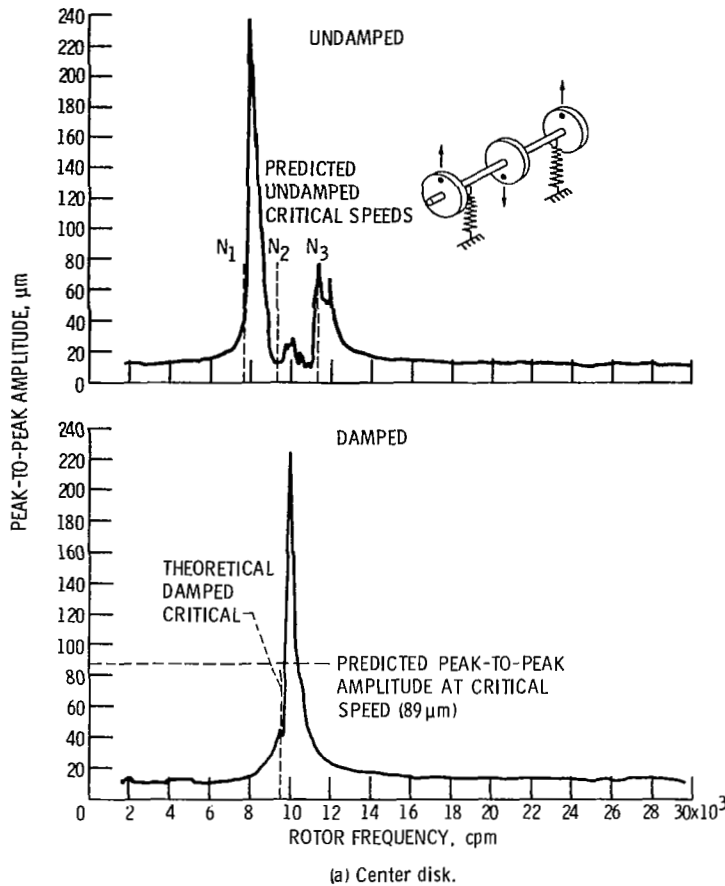
Figure 9. – Comparison of rotor response for undamped and damped
conditions. Type I unbalance distribution; unbalance, U = 0.93
gram-centimeter.

The undamped rotor exhibited three distinct amplitude buildups at frequencies close
to the ones predicted by the critical speeds program of reference 7. The maximum un-
damped resonant amplitude occurred at 8100 cycles per minute. The type of unbalance
distribution used in this trial would normally excite the first and third bending critical
speeds, as can be seen from the mode shapes of figure 7. Therefore, it is reasonable to
expect larger amplitudes to occur at resonant frequencies corresponding to those modes.
It should be pointed out that, even though no external squeeze-film damping was present
in this trial, it is obvious that some amount of damping is present in the oil-lubricated
ball bearings. The maximum amplitude predicted by an unbalance response program,
for a ball bearing damping of 3500 newton-seconds per meter, is 381 micrometers at
7500 cycles per minute.

The lower portion of figure 9(a), for the test where oil-squeeze-film dampers were
activated, shows one distinct buildup in rotor amplitude instead of three. The mode
shape for this damped critical, occurring at 10 000 cycles per minute, was similar to the

13

(b) Disk 3.
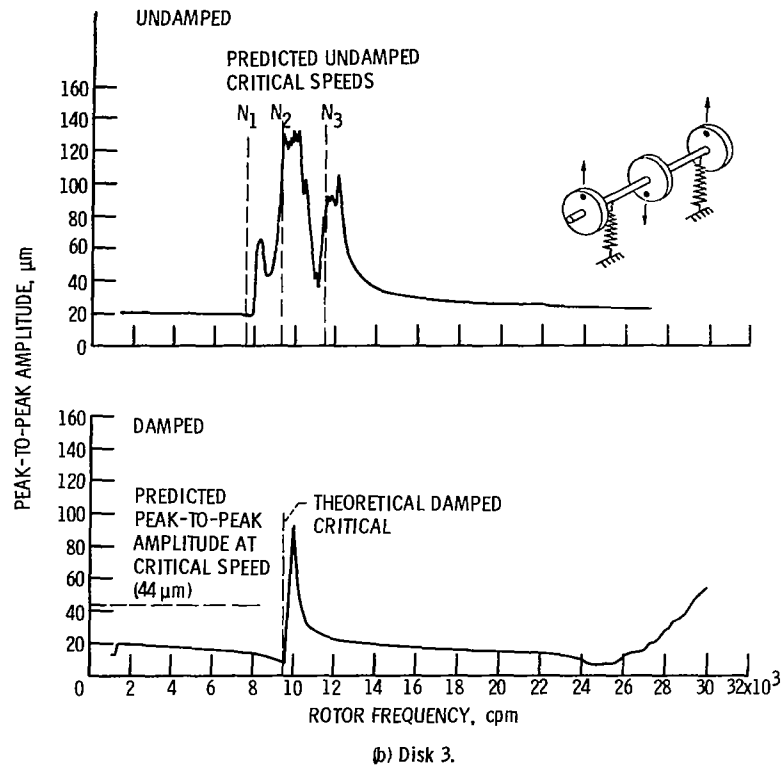
Figure 9. – Concluded.

one at the third bending critical (fig. 7). The maximum peak-to-peak amplitude, when dampers were activated, was 216 micrometers, and this obviously was not a significant improvement. The unbalance-response program, however, predicted a maximum amplitude of only 85 micrometers at 9600 cycles per minute. The agreement between experiment and theory for this unbalance distribution was obviously not very good. Because of the large rotor excursions exhibited for unbalances of 0.93 and 1.67 gram-centimeters, tests at greater unbalances were not attempted to avoid damaging rig components, such as the labyrinth seals located at the bearing supports.

Figure 9(b) is the filtered response of disk 3, located at the end opposite the turbine drive. Again, for the undamped run, there are three distinct amplitude buildups, which are at frequencies approximating those predicted by the undamped critical speeds program. The end disk tends to move out to amplitudes greater than indicated on this plot; however, the damper journal can move out only as far as the clearance in the bearing will permit, and this movement is approximately 127 micrometers. This may account for the jagged appearance of the trace at the second and third critical speeds. With the activation of the dampers, the trace smooths out; again the theoretical prediction of the maximum amplitude of 44 micrometers is low.

14

Low-speed measurements made at a number of places along the shaft from bearing to bearing indicated a bowing or warping of the shaft. The maximum amount of warp or bow at either side of the center disk was approximately 10 to 13 micrometers. This shaft runout can be seen in all the plots. The in-line, out-of-phase unbalance distribution was inadvertently placed in a plane only 40° away from the plane of the residual warp. This then could account for the shaft having a strong tendency to bend a greater amount in this plane than in any other.

Figure 10. - Comparison of rotor response for undamped and damped conditions. Type II unbalance distribution; unbalance, U, 0.62 gram-centimeter.

The rotor responses shown in figure 10 are for an in-line, alternating-phase distribution for two disks only; the center disk did not have an unbalance weight (see inset). This type of unbalance distribution should have excited the second mode shape (see fig. 7). The undamped response, however, is similar to the previous in-line alternating phase response for three disks. Activating the oil-film dampers significantly reduced the resonant amplitude. An amplitude of approximately 36 micrometers was recorded at 9700 cycles per minute, whereas the unbalance response program predicted an amplitude of 20.3 micrometers at 10 000 rpm.
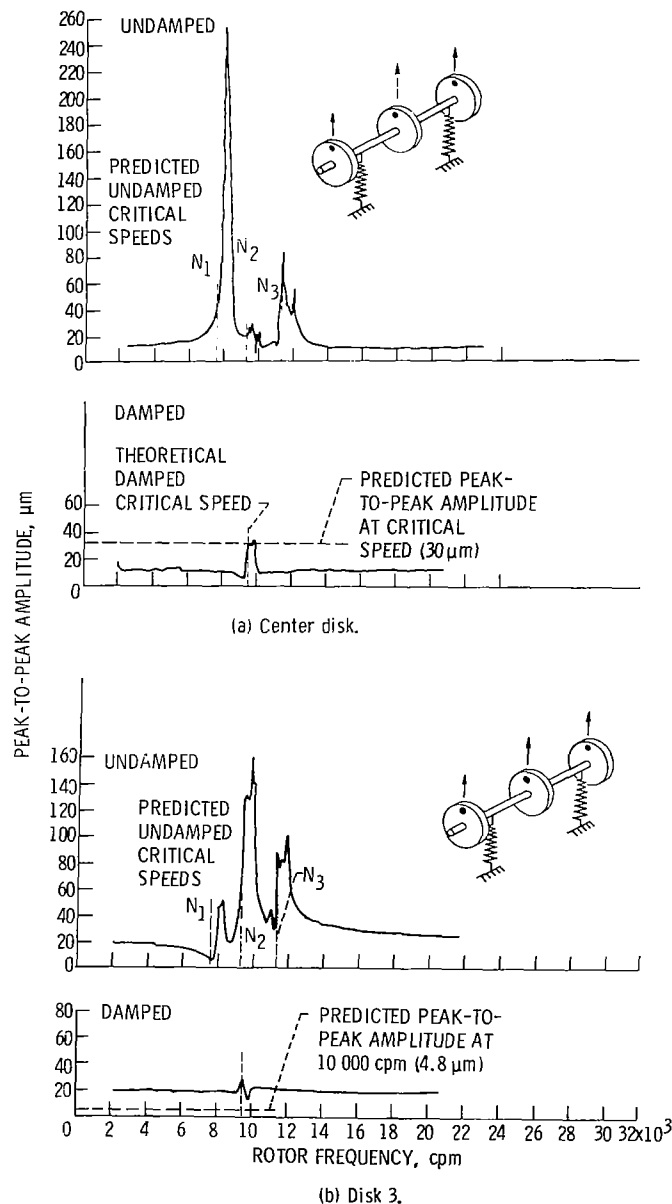
Figure 11. - Comparison of rotor response for undamped and damped conditions. Type III unbalance distribution; unbalance, U, 0.93 gram-centimeter.

A total unbalance weight of 0.154 gram is quite small compared with a rotor weight of 4.54 kilograms. It is apparent from these undamped rotor tests that this small amount of unbalance is not capable of inducing rotor bending in the classical mode shapes depicted in figure 7, particularly when both a residual bow and some residual unbalance (fig. 8) are present.

The unbalance distribution used to generate the experimental responses shown in figures 11(a) and (b) for the center and end disk, respectively, is an in-line, in-phase distribution using all three disks (see inset). The oil-squeeze-film dampers cause a reduction in the peak-to-peak amplitude of over 80 percent. The predicted amplitude at the center disk of 30 micrometers at 9500 rpm for the damped rotor compares favorably with a measured amplitude of approximately the same magnitude at a rotor frequency of 9600 cycles per minute.

The response for an in-line, in-phase unbalance distribution applied to the test rotor correlated well with the predicted response at very small unbalances, as shown in figure 11. It was decided to examine the response for much greater magnitudes of unbalance. In figure 12 the actual and theoretical rotor responses are compared. It is apparent in figure 12(a), which is the peak-to-peak amplitude of the center disk, that squeeze-film dampers located at the bearings of a long, slender rotor are going to have little effect on attenuating midspan excursions. The agreement between the actual response and the predicted is quite good for both the amplitude and the frequency at which resonance occurs.

The theoretical response program will predict, with considerably accuracy, the amplitudes, phase angles, and forces transmitted if the input data, such as support flexibility and damping, are accurate. In this case the matchup is close. Stiffnesses of the centering springs were carefully measured, and this value was entered in the program as input. Damping coefficients were calculated from theory and for this case agreed quite well with measured values, at least at the resonant frequency. Damping values of 6300 newton-second per meter shown on the plots were calculated for a concentrically positioned damper journal.

It should be noted here that the recorded amplitudes of motion and transmitted forces were in the vertical or Y direction. Response was also measured in the X direction and appeared similar to Y measurements. The value of radial clearance used in calculating the damping for the theoretical unbalance response was 63.5 micrometers, which was also the measured assembled clearance.

In figures 12(b) and (c), considerable disagreement is apparent between the measured amplitudes of motion and the theoretical for both the end disk and the damper journal. The theoretical response is much greater than the measured response at frequencies above 10 000 cycles per minute. It is not exactly clear why such diagreement exists at the higher unbalances of 10.6 and 15.1 gram-centimeters. The rotor end and damper journal, opposite the turbine, deflect much less than predicted. The reason for this may
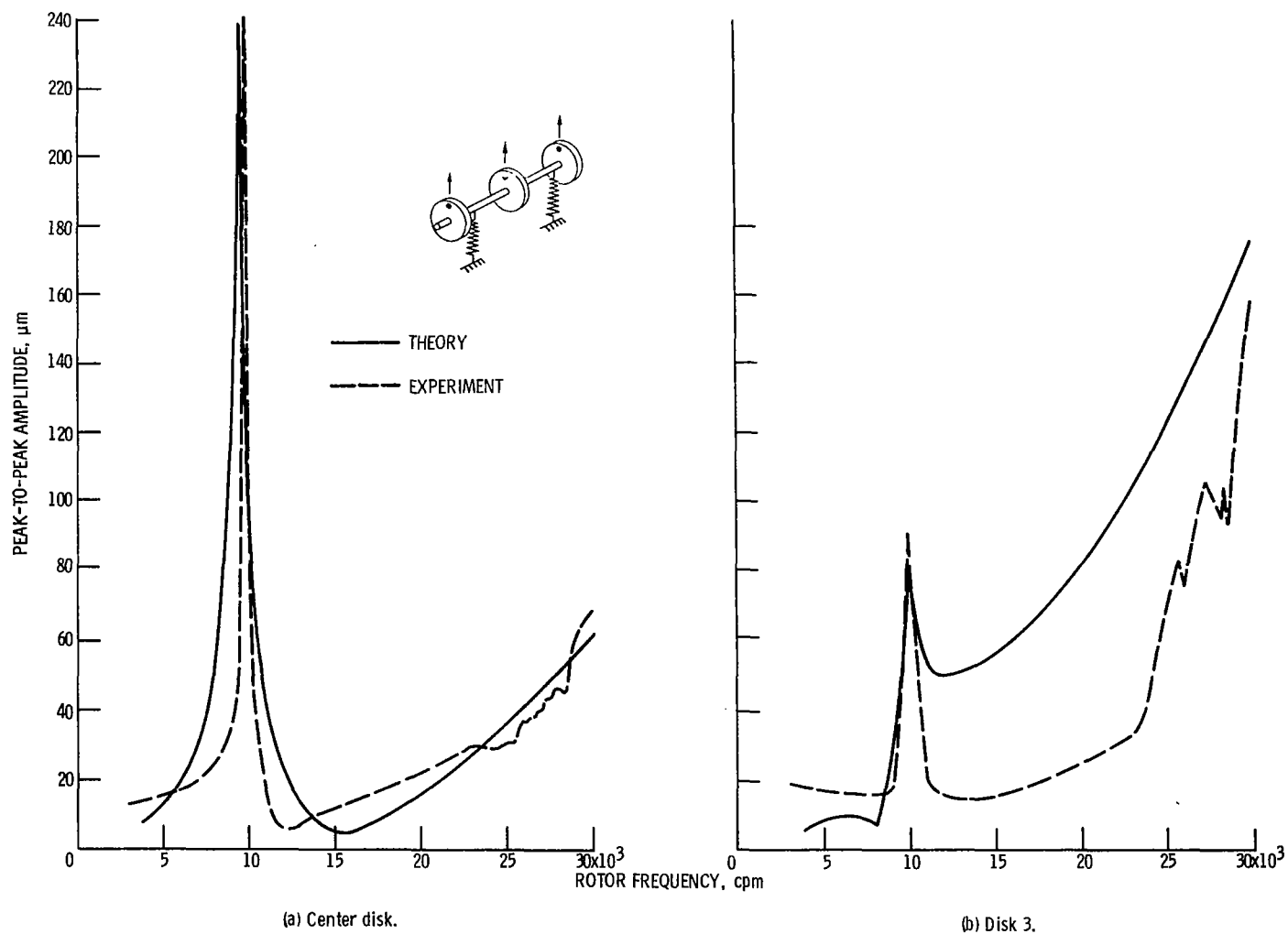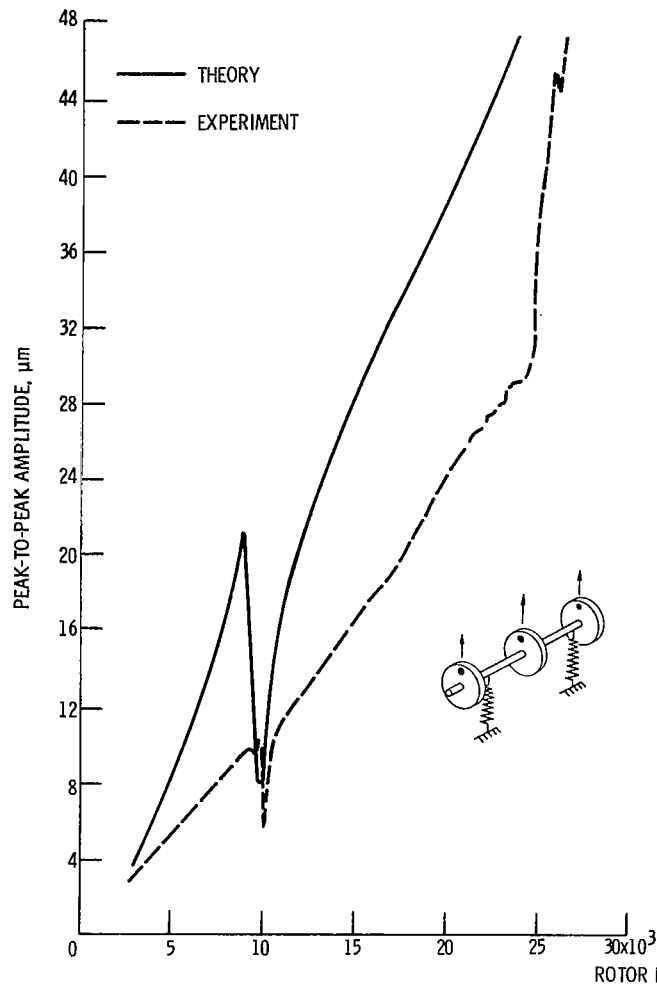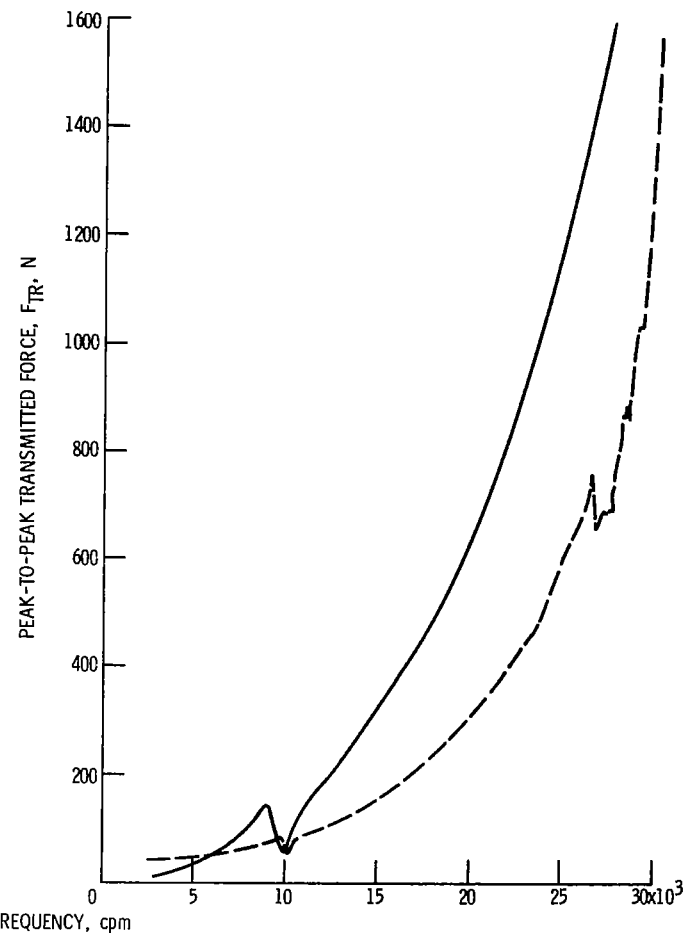
17

(a) Center disk.

(b) Disk 3.

Figure 12. - Comparison of experimental and theoretical damped rotor response. Type III unbalance distribution; unbalance, U, 10.6 gram-centimeters; theoretical elastic force, K, 23.63×10^5 newtons per meter; damping coefficient, $B_{\eta=0}$, 6300 newton-seconds per meter; radial clearance, C_R, 63.5 micrometers.

(c) Damper journal bearing 2.

(d) Transmitted force at bearing 2.

Figure 12. - Concluded.

be the noncylindrical shape of the damper bearing (see fig. 5). The walls of the bearings were thinner where distance probes were mounted. It is possible that this member was flexing asymmetrically, particularly with the higher rotating unbalance, and therefore the absolute damper journal motions measured were less than if the damper bearing were perfectly rigid. The transmitted force also would be less in the actual system, since it is a function of the sum of elastic and damping forces, both of which, in turn, are functions of the displacement.

The photographs of figure 13(a) show the damper journal orbital motion. The pictures on the left are for an undamped system, with the damper oil supply off. The pictures on the right are for identical conditions of unbalance, magnitude, and frequency except that oil was supplied to the dampers. It should be pointed out that these pictures are of the unfiltered signals, and, therefore, Lissajous patterns of orbital motion are generated which can be nonsynchronous as well as synchronous. The large orbit of the undamped journal motion at 9020 cycles per minute had a synchronous critical frequency with a peak-to-peak amplitude of 96.4 micrometers. The amplitude, frequency trace of figure 13(b) is a filtered signal made at the same time. The picture of the orbit was snapped while the rotor was approaching the second critical speed of 9600 rpm. The undamped trace of figure 13(b) shows only resonances which are synchronous. Some of the multiple harmonics that occur in a lightly damped ball-bearing-supported rotor can have large amplitudes that can be quite destructive. These motions would not be seen at all if only the filtered trace were being observed. The Lissajous pattern at 25 710 rpm in figure 13(a) has one inward loop; this signifies a multiple harmonic having a frequency twice that of the rotor speed. This orbit is a result of the gravity vector of a horizontally supported rotor superimposed on the unbalance whirl vector (ref. 12).

The noteworthy point to be made concerning these pictures is that oil-squeeze-film damping is very effective in attenuating the motions of both synchronous and nonsynchronous whirl. The amplitudes of motion for the damped tests were all less than those for the undamped tests. This fact is apparent in the filtered amplitude frequency traces shown in figure 13(b). The damped trace is superimposed on the undamped for a direct comparison of the synchronous motions.

Oil-Squeeze-Film Damping

Presented in figures 14 to 16 are oil-squeeze-film damping coefficients, the force transmitted through the oil film, and the eccentricity ratio, all plotted as functions of rotor frequency. Eccentricity ratio, as defined here, is the average of the peak journal displacements in the X-Y plane divided by the radial clearance in the damper. Table I contains a summary of average damping coefficients at different magnitudes of unbalance and types of unbalance distributions.
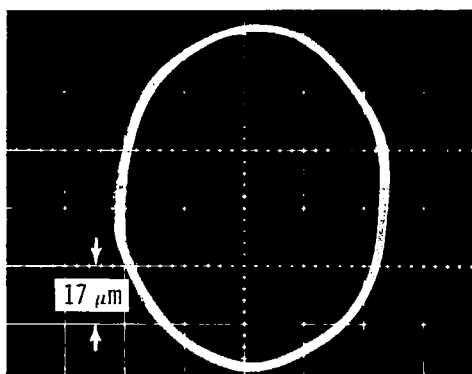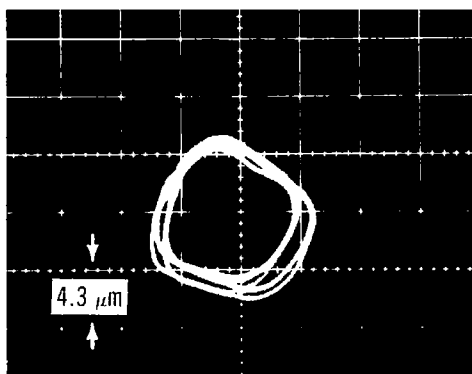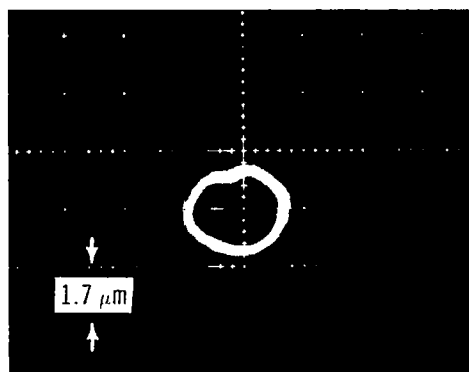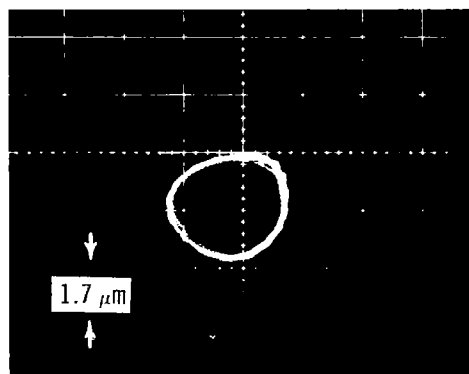
9020 rpm
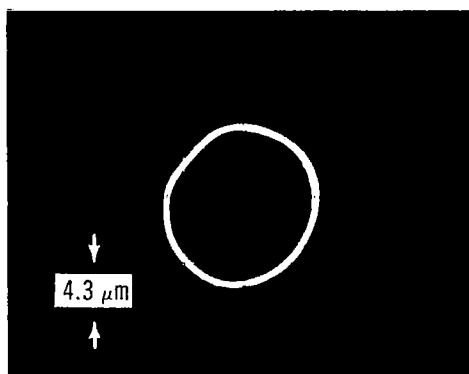
9030 rpm
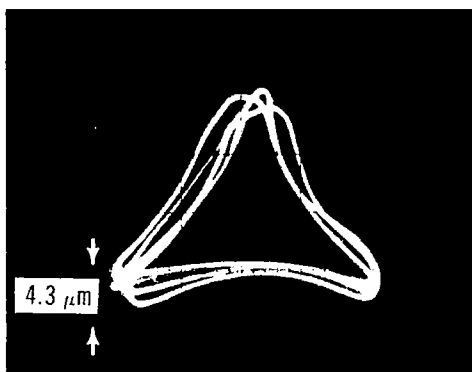
14 820 rpm

18 600 rpm
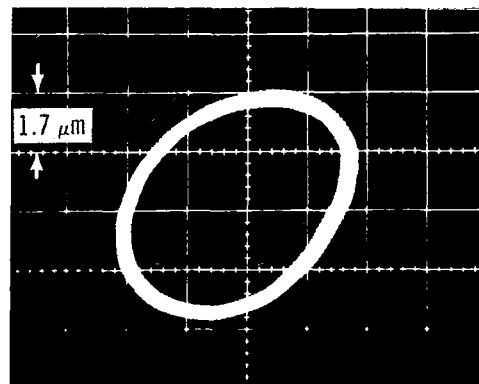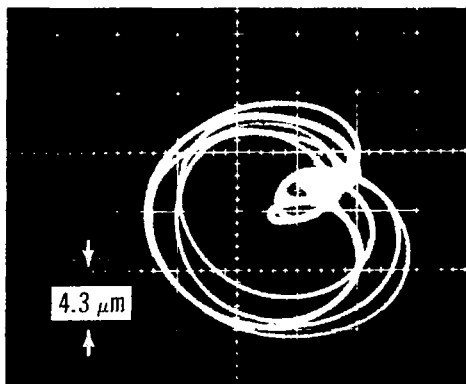
UNDAMPED RESPONSE   DAMPED RESPONSE
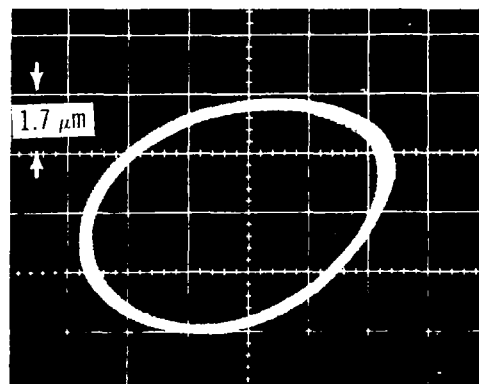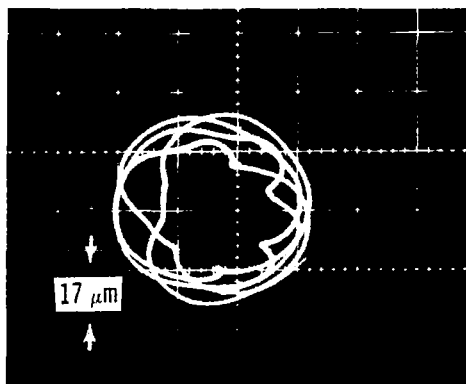
(a) Orbital motion.

Figure 13. - Orbital motion of damper journal (bearing 2) with and without oil and corresponding amplitude, frequency response. Type I unbalance distribution; unbalance, U, 0.93 gram-centimeter; radial clearance, C_r, 63.5 micrometer; oil flow, 5.15×10^{-4} cubic meter per minute; supply pressure, 0.19 megapascal.
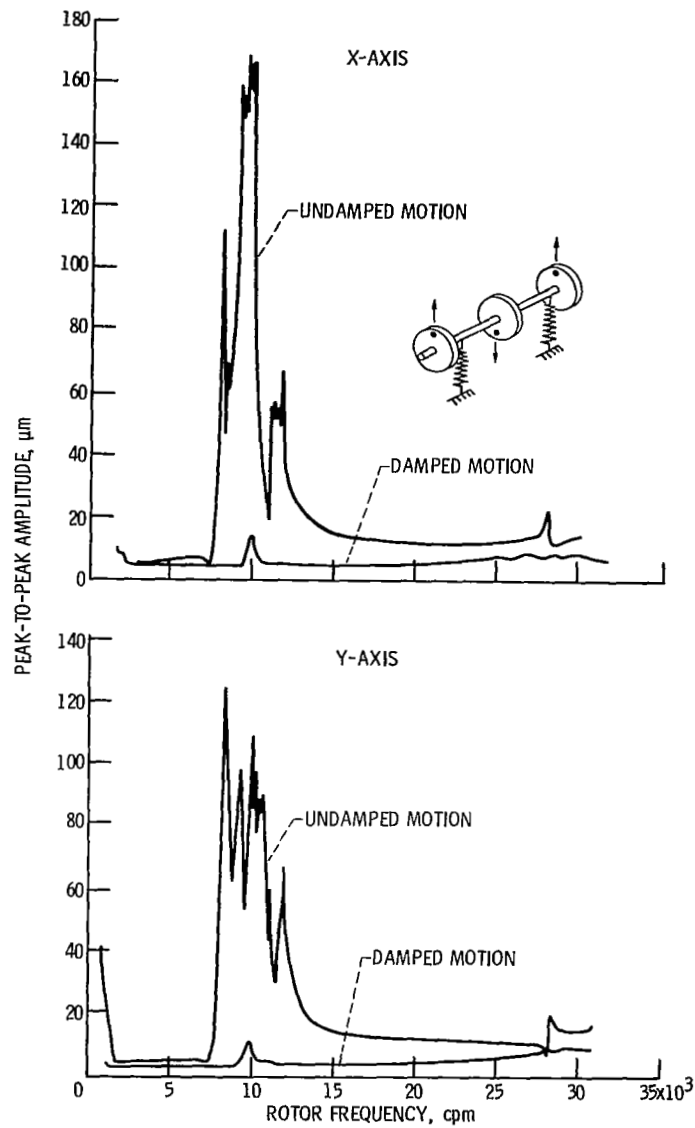
21
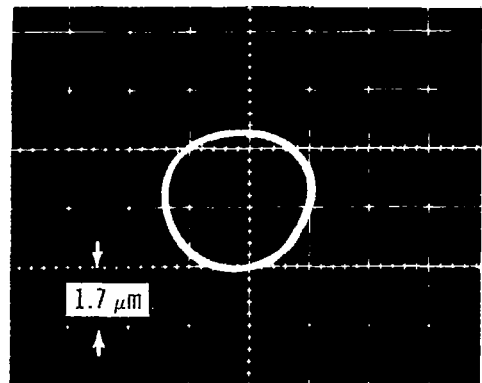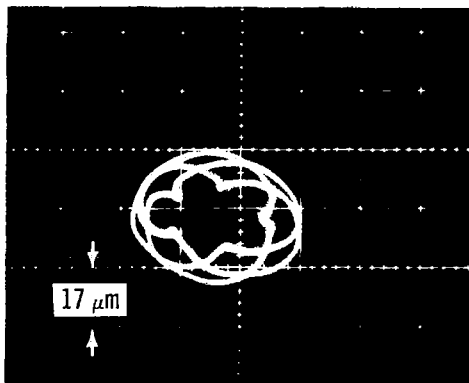
21 810 rpm

25 710 rpm

29 500 rpm

UNDAMPED RESPONSE   DAMPED RESPONSE

(a) Concluded.

Figure 13. - Continued.

(b) Amplitude, frequency response.

Figure 13. – Concluded.

The experimental values obtained in this investigation are averages calculated from amplitudes, forces, and phase angles measured in the X-Y plane. The relation of the force transducers and displacement sensors is shown in the schematic of figure 6. Because displacement sensors and force transducers were not located in the same transverse planes, the phase angles measured had to be adjusted by 45°. This probably resulted in some error in calculating the damping coefficients, but because the orbits were nearly circular (see fig. 13), the error introduced was not large. The straight lines plotted in figures 14 to 16 are the values of theoretical damping for a concentrically positioned journal (eccentricity ratio $\eta = 0$) and a 180° film.

The experimental values of transmitted force and eccentricity ratio plotted in these figures are also averages of values measured in the X-Y plane. These values are compared with those obtained in the unbalance response program.

Values of damping coefficient were obtained by measuring the force transmitted through the oil film to the damper bearing F_{TR}, the displacement of the damper journal e, the angle by which the displacement lags the exciting force (acts 180° from transmitted force) φ, the rotor frequency ω, and the amplitude of the transmitted force F_0.

The derivation of the equations used in the data reduction is given in the appendix; the equations are as follows:

Damping coefficient:

$$B_{x,y} = \frac{\left(F_0\right)_{x,y} \sin \varphi_{x,y}}{e_{x,y}\omega}$$

Stiffness coefficient:

$$K_{x,y} = \frac{\left(F_0\right)_{x,y} \cos \varphi_{x,y}}{e_{x,y}}$$

Stiffness coefficients are not presented in this report. The values calculated from this expression would depend on the cosine of the measured phase angles. The accuracy of the angle near 90° is approximately $\pm 1^O$. This error is not serious when the sine of the angle is taken, since the sine does not vary significantly for 2^O when near 90°. However, the cosine does vary significantly even for 2^O, and consequently there is a significant error introduced in calculated values of the oil-film stiffness coefficient.

Theoretical damping coefficients plotted in figures 14 to 16 were calculated from the following equation:

$$B = \frac{\pi \mu R L^3}{C_R^3 (1 - \eta^2)^{3/2}}$$

where μ is oil viscosity, R is journal radius, L is journal land length, C_R is radial clearance (diametral clearance/2), and η is the conventional journal eccentricity ratio, defined as a static deflection e_0 divided by the radial clearance C_R. For the theoretical damping coefficients calculated in figures 14 to 16, η is zero. Dynamic eccentricity
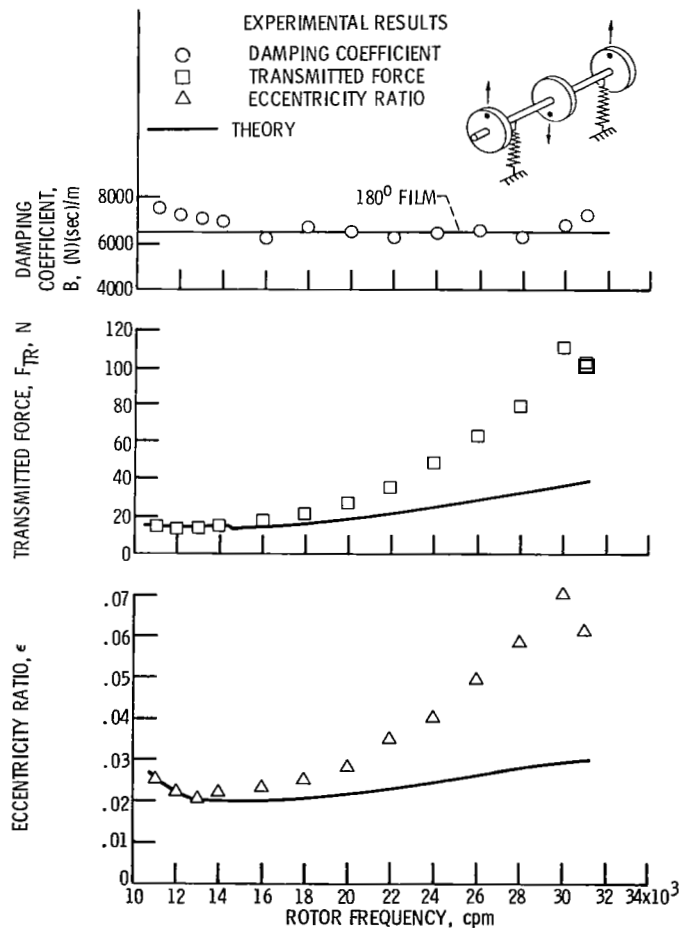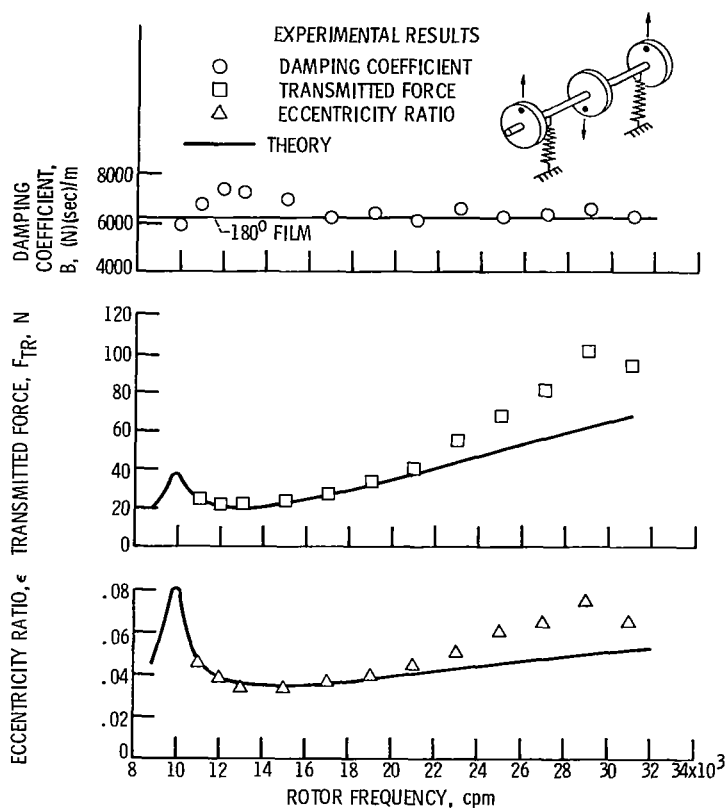

(a) Unbalance, U, 0.93 gram-centimeter.

Figure 14. - Comparison of theoretical and experimental damping coefficients, transmitted forces, and eccentricity ratios as functions of rotor frequency. Type I unbalance distribution.

25

ratio ϵ plotted in these figures is defined as the radius of the orbit e divided by the radial clearance C_R. This equation is derived from the Reynolds lubrication equation for the case of a 180° film (cavitated bearing) by using short-bearing theory (ref. 10).

Results plotted in figures 14(a) and (b) are for an in-line, alternating-phase unbalance distribution. The total unbalances were 0.93 and 1.67 gram-centimeter, respectively. Average values for the experimental damping coefficient were 6740 and 6531 newton-second per meter, as compared with values of 6492 and 6213 newton-second per meter for the theoretical, 180° film. In all the tests the damper oil supply pressure was set at 0.19 megapascal, and the flow rate was 5.15×10^{-4} cubic meter per minute. The fact that the experimental damping coefficients over the frequency range were slightly higher than the theoretical indicated that at certain conditions of speed and load the actual oil-film extent in the damper may be slightly greater than 180°.

The results plotted in figure 15 are for an in-line, alternating-phase unbalance distribution for the two end disks only, designated unbalance type II. The experimental values of damping coefficients have somewhat more scatter than the previous data; however, the values do not deviate too much from those for the theoretical 180° cavitated film predicted by short-bearing theory. Average values are compared in table I. Ex-

(b) Unbalance, U, 1.67 gram-centimeters.

Figure 14. - Concluded.
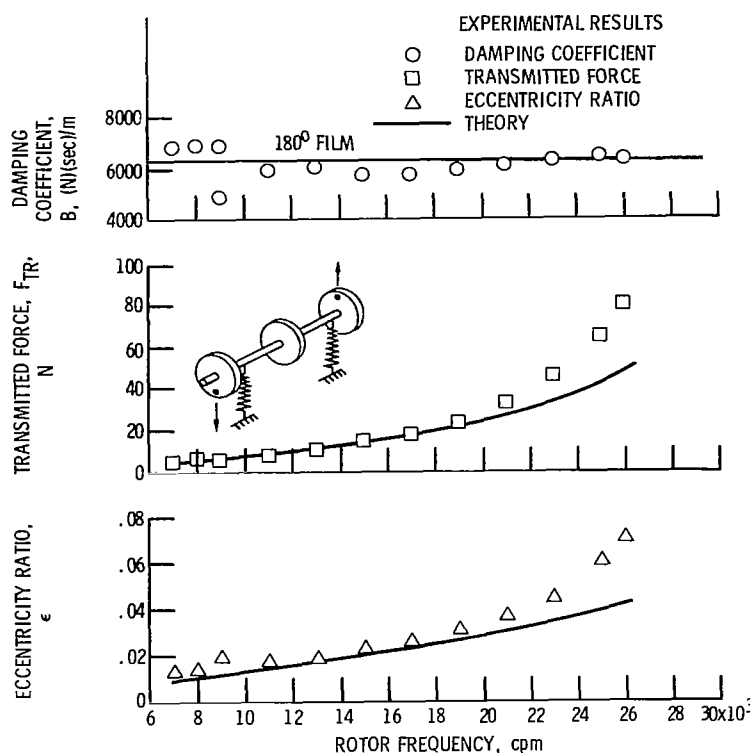
Figure 15. - Comparison of theoretical and experimental damping coefficients, transmitted forces, and eccentricity ratios as functions of rotor frequency. Type II unbalance distribution.

(a) Unbalance, U, 0.62 gram-centimeter.

perimental values of damping coefficient deviate from theory most at rotor frequencies near the critical, which is approximately 9600 cycles per minute. Phase angles approaching the critical frequency change very rapidly, and, therefore, the angles are subject to more error than those angles measured at frequencies greater than the critical frequency. Rotor orbits at these frequencies are also elliptical.

Agreement between theory and experiment for the transmitted force and the eccentricity ratio is quite good throughout most of the frequency range. Experimental values tend to increase at a faster rate at higher rotor speeds. Evidence indicates that a fourth bending critical is being approached.

In figure 16 damping coefficient, transmitted force, and eccentricity ratio are plotted as functions of rotor frequency. The unbalance distribution used in the three disks was an in-line, in-phase distribution, designated type III. Magnitudes of total unbalance varied from 0.93 to 15.1 gram-centimeter. The experimental values vary from 6.8 percent below to 9.2 percent above the predicted values. The trend, however, indicates experimentally determined damping coefficients for these series of tests are in excellent agreement with values calculated from short-bearing theory for a 180°, cav-

EXPERIMENTAL RESULTS

○ DAMPING COEFFICIENT
□ TRANSMITTED FORCE
△ ECCENTRICITY RATIO
— THEORY
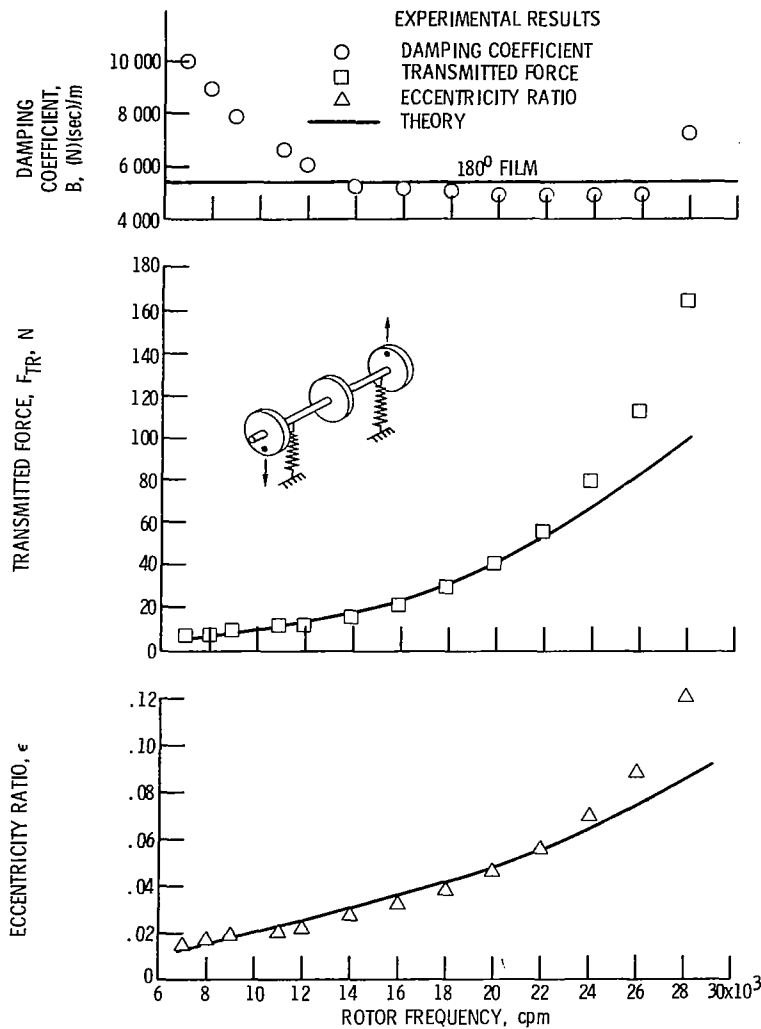
(b) Unbalance, U, 1.11 gram-centimeters.

Figure 15. - Continued.

itated film. Experiments also indicate that damping coefficients are not a strong function of dynamic eccentricity ratio but, in general, remain fairly constant. Similar results are presented in reference 13; that is, squeeze-film damping coefficients, although greater than predicted by 180° film theory, remained fairly constant at dynamic eccentricity ratios varying from 0. 03 to 0.4 for an end fed damper with a length-diameter ratio of 0.34.

The data plotted in figures 16(d), (e), and (f) are for total unbalances of 4.97, 10.6, and 15. 1 gram-centimeters, respectively. The resulting higher dynamic eccentricity ratios were expected to result in higher damping coefficients. This did not occur; in fact, an opposite trend was observed, in that damping coefficients actually decreased. Also, a hydrodynamic instability was induced. This type of operation is referred to in
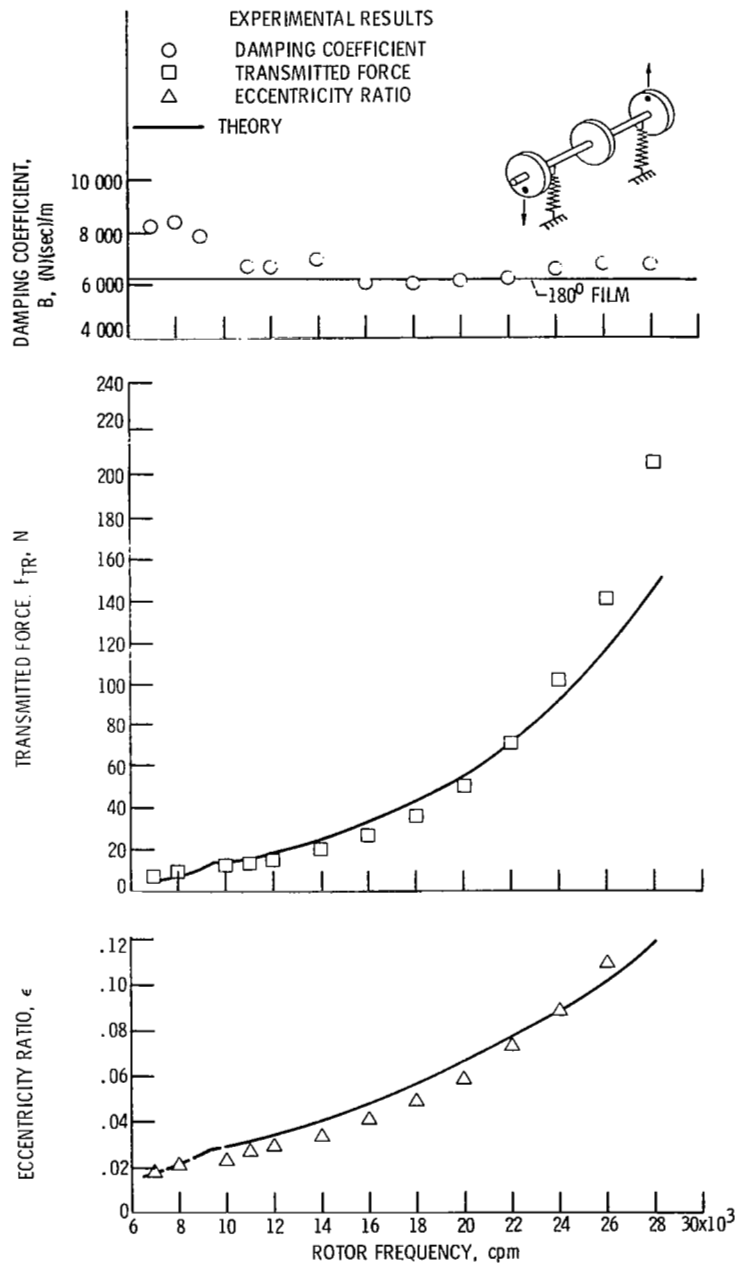
28

(c) Unbalance, U, 1.5 gram-centimeters.

Figure 15. - Continued.

the literature (refs. 14 and 15) as bistable operation. Briefly, it is operation of the damper journal in a stable condition at either of two eccentricity ratios. The region of frequency where this instability occurred is shown in figures 16(e) and (f). The rapid increase in journal amplitude is also shown at approximately 25 000 rpm in figure 12(c). A region is indicated since the bistable phenomenon noted did not always occur at exactly
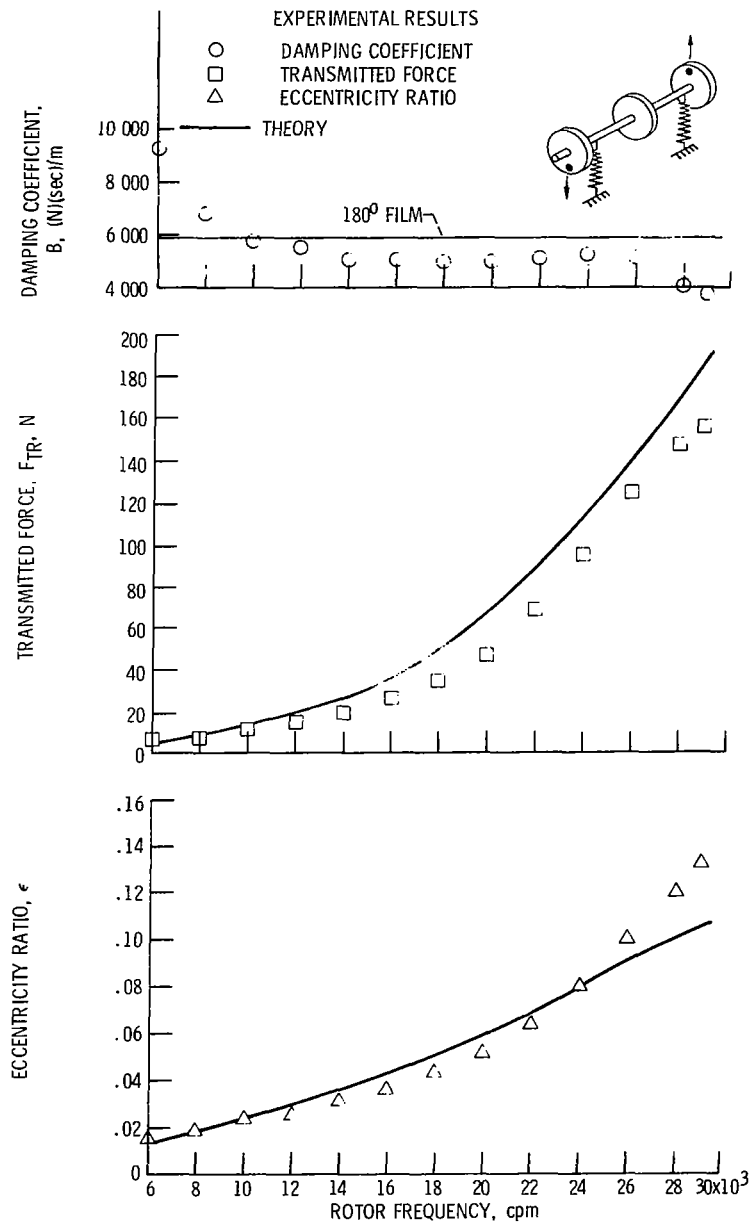
29

EXPERIMENTAL RESULTS
○   DAMPING COEFFICIENT
□   TRANSMITTED FORCE
△   ECCENTRICITY RATIO
——   THEORY

(d) Unbalance, U, 3.3 gram-centimeters.

Figure 15. – Concluded.

the same frequency in subsequent trials. It is not the purpose of this investigation to examine non-steady-state behavior other than to note its dramatic effect in the reduction of the damping coefficient. The oil flow to the damper increased at frequencies approaching the bistable region. It is postulated that the damper at this juncture became starved, and the oil film ruptured. This would account for the decrease in damping coefficients above the instability region.
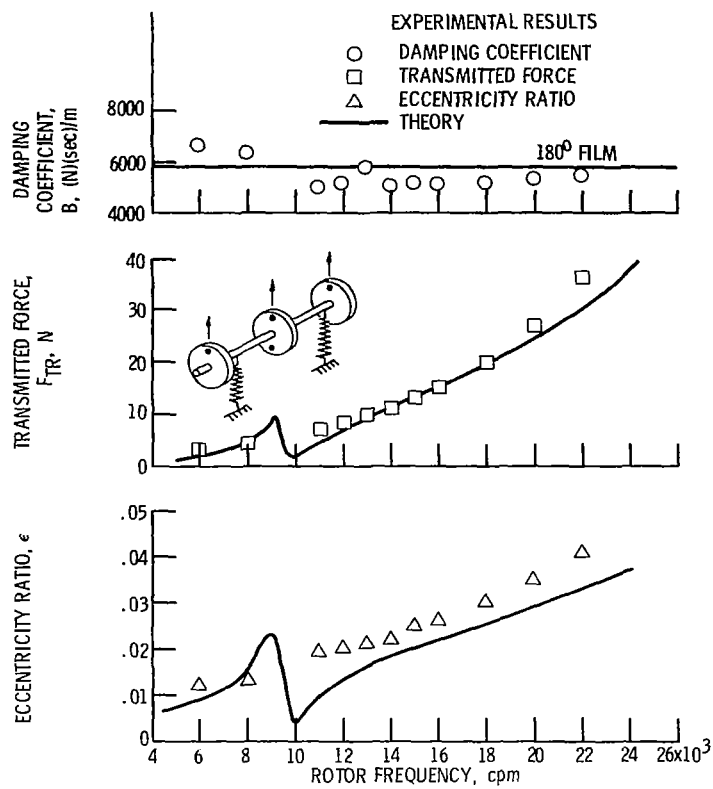
(a) Unbalance, U, 0.93 gram-centimeter.

Figure 16. - Comparison of theoretical and experimental damping coefficients, transmitted forces, and eccentricity ratios as functions of rotor frequency. Type III unbalance distribution.
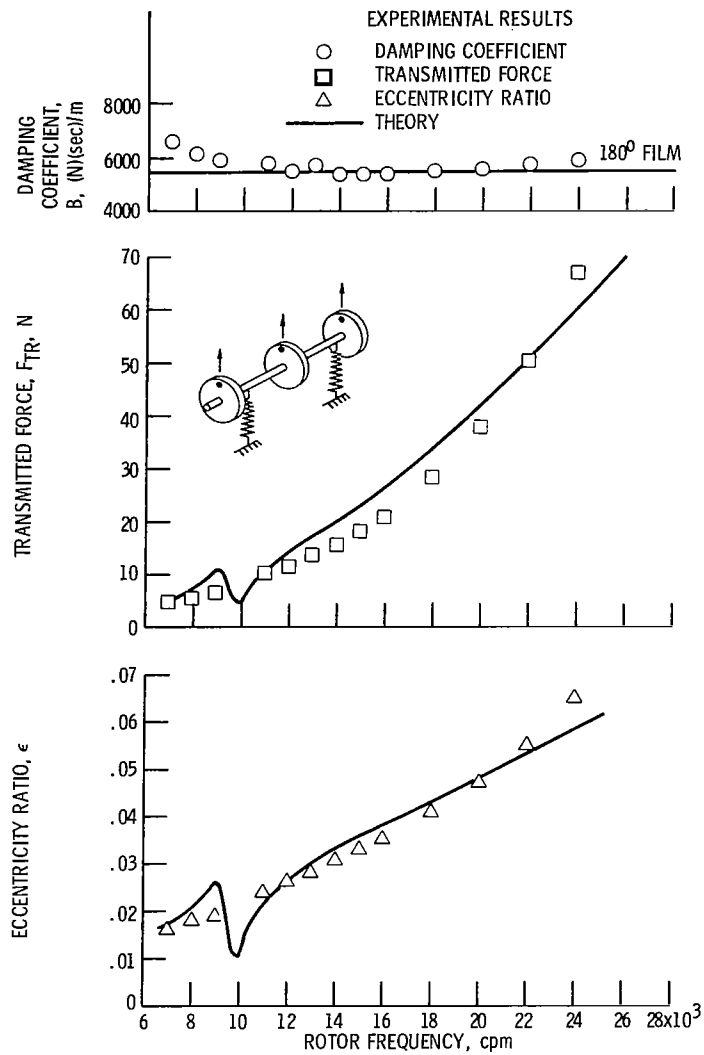
31

(b) Unbalance, U, 1.67 gram-centimeters.
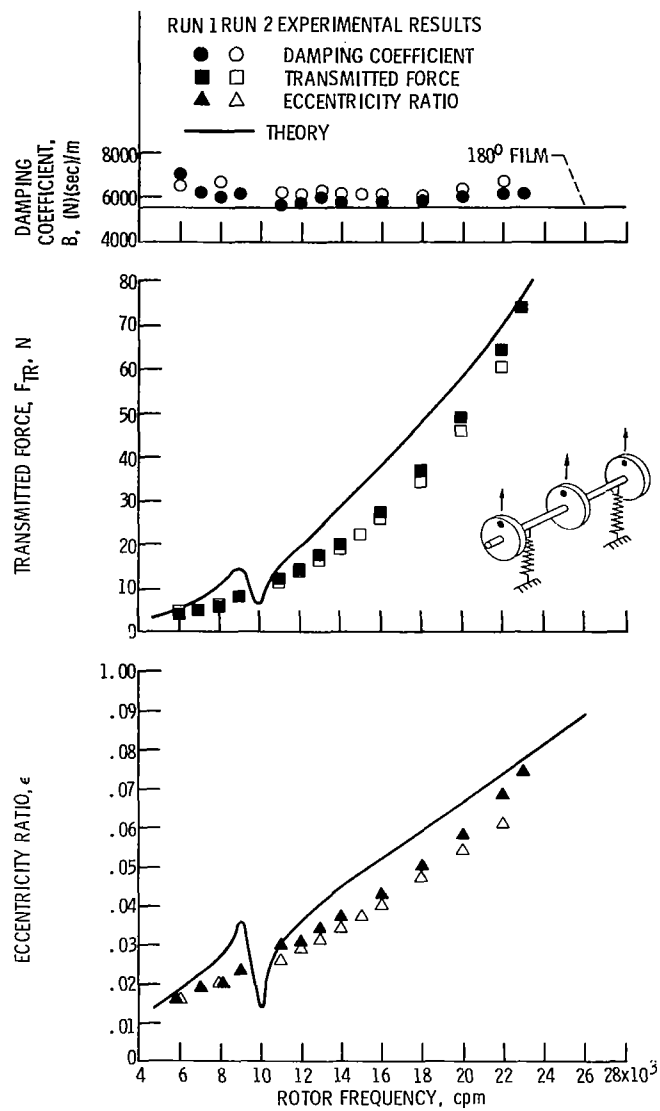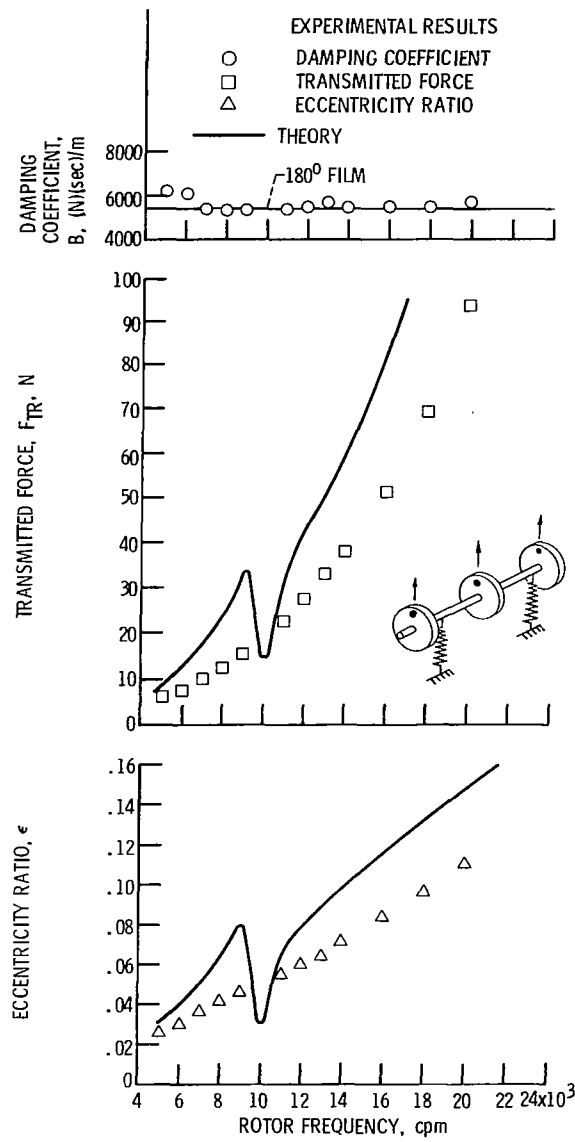
Figure 16. – Continued.

(c) Unbalance, U, 2.25 gram-centimeters.

Figure 16. - Continued.

EXPERIMENTAL RESULTS
○ DAMPING COEFFICIENT
□ TRANSMITTED FORCE
△ ECCENTRICITY RATIO
—— THEORY

(d) Unbalance, U, 4.97 gram-centimeters.

Figure 16. - Continued.

EXPERIMENTAL RESULTS
○ DAMPING COEFFICIENT
□ TRANSMITTED FORCE
△ ECCENTRICITY RATIO
—— THEORY

(e) Unbalance, U, 10.6 gram-centimeters.

Figure 16. - Continued.

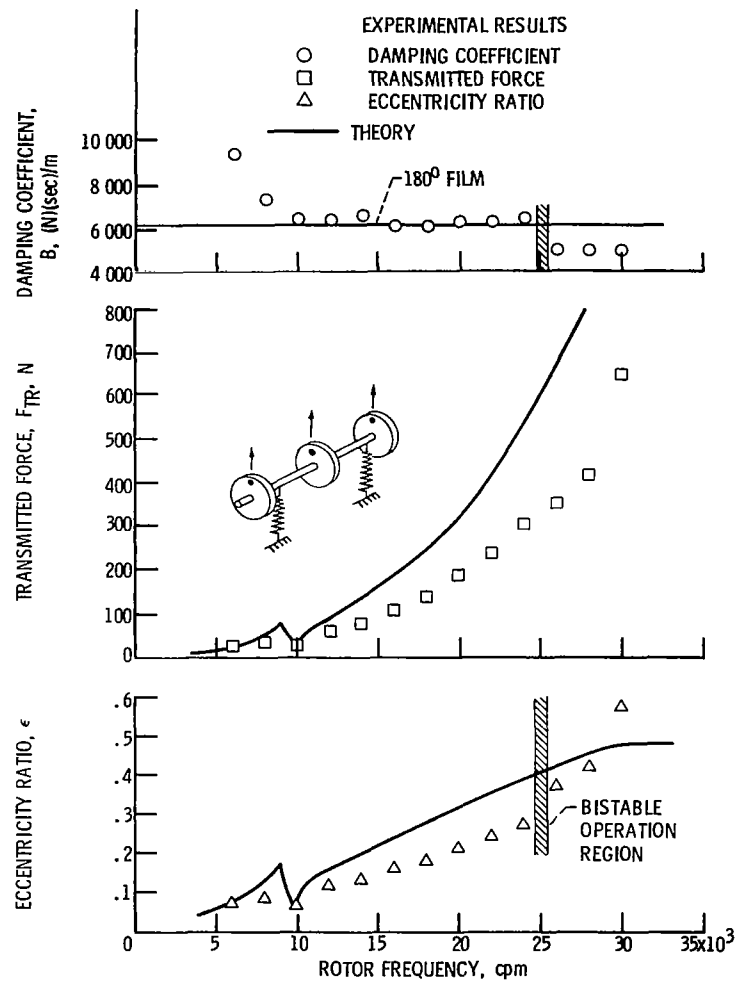EXPERIMENTAL RESULTS
○ DAMPING COEFFICIENT
□ TRANSMITTED FORCE
△ ECCENTRICITY RATIO
— THEORY
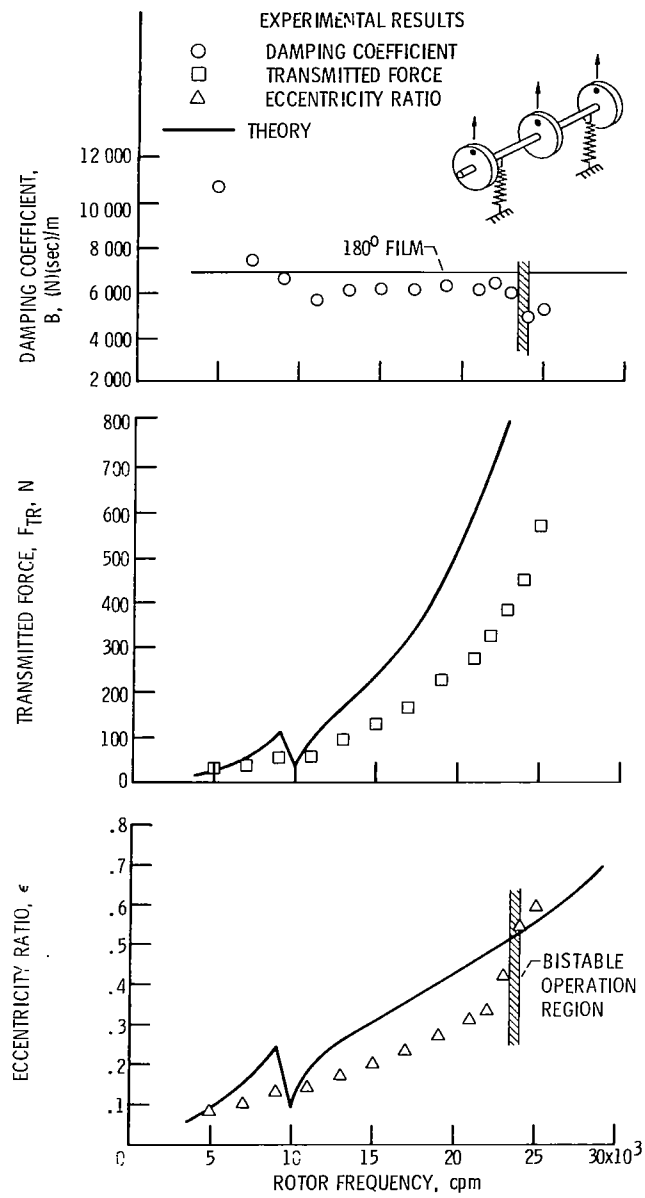
(f) Unbalance, U, 15.1 gram-centimeters.

Figure 16. – Concluded.

SUMMARY OF RESULTS

Experimentally determined values of squeeze-film damping coefficients were in good agreement with theoretical values calculated from equations derived by the short-bearing approximation for a 180° film and a concentrically positioned journal. Values remained fairly constant at rotor frequencies up to 31 000 cycles per minute.

Central-feed-groove oil-squeeze-film dampers, located at the bearings, were most effective in reducing amplitudes of motion at the rotor ends. They were, however, less effective in attenuating amplitudes of motion at the rotor center. A reduction in amplitude of 88 percent was observed for an unbalance moment of 0.93 gram-centimeter distributed in line and in phase over three disks.

When oil-squeeze-film dampers were activated, for an in-line, alternating-phase unbalance distribution, three distinct resonant amplitudes were reduced to only one. The mode shape for this one corresponded to the third bending critical speed.

The oil-squeeze-film dampers were effective in reducing the amplitudes of motion for nonsynchronous whirl as well as synchronous.

An unbalance-response computer program was found to be quite accurate in predicting the response of the three-disk experimental rotor used in this investigation. The discrepancies that did occur apparently were due to the presence of a residual bend in the rotor having a shape similar to that which occurs at the first critical speed. The placement of weights in a line and near the plane of residual bend induced greater bending than would probably have occurred with a straighter shaft. Conversely, locating the center weight 180° from the weights in the two end disks resulted in the rotor not bending as much as predicted by theory.

Unbalances of 10.6 and 15.1 gram-centimeters arranged in line and in phase in all three disks produced an instability in the rotor referred to as bistable operation. Damping coefficients were reduced significantly at frequencies greater than the onset frequency. Damper oil flow rates increased, probably as a result of the higher damper journal eccentricities and increased hydrodynamic pumping.

With the undamped rotor, resonant amplitudes occurred at frequencies slightly greater than those predicted by a critical-speed, mode-shape program.

Lewis Research Center,
  National Aeronautics and Space Administration,
    Cleveland, Ohio, July 28, 1977,
      505-04.

APPENDIX - DERIVATION OF DATA REDUCTION EQUATIONS

The force transmitted through the oil film to the damper bearing, and measured by the force transducers, is equal to the sum of the elastic force, the dissipative or damping force, and the oil-film inertial force:

transmitted force = elastic force + damping force + inertial force

Because the volume of oil in the squeeze film is so small, the inertial force can be neglected, and

$$\left(F_{TR}\right)_{x,y} = K_{x,y}(x,y) + B_{x,y}\frac{d(x,y)}{dt} \tag{A1}$$

It is assumed that the journal precesses about the bearing center in an elliptical orbit and the motion is harmonic:

$$\left.\begin{aligned} x &= e_x \cos \omega t \\ y &= e_y \sin \omega t \end{aligned}\right\} \tag{A2}$$

$$\left.\begin{aligned} \frac{dx}{dt} &= -e_x \,\omega \sin \omega t \\ \frac{dy}{dt} &= e_y \,\omega \cos \omega t \end{aligned}\right\} \tag{A3}$$

Let $\left(F_0\right)_{x,y}$ be the amplitudes of the transmitted force in the x and y directions, respectively; then

$$\left.\begin{aligned} F_x &= \left(F_0\right)_x \cos(\omega t + \varphi_x) \\ F_y &= \left(F_0\right)_y \sin(\omega t + \varphi y) \end{aligned}\right\} \tag{A4}$$
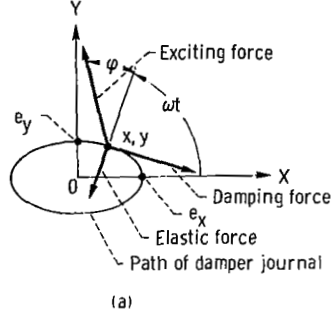
Substituting equations (A2), (A3), and (A4) in (A1), we obtain

$$F_x = K_x e_x \cos \omega t - B_x e_x \omega \sin \omega t = \left(F_0\right)_x \cos(\omega t + \varphi_x) \tag{A5}$$

and

$$F_y = K_y e_y \sin \omega t + B_y e_y \omega \cos \omega t = \left(F_0\right)_y \sin(\omega t + \varphi_y) \qquad \text{(A6)}$$

where φ_x and φ_y are the angles by which the displacement lags the exciting force (see sketch (a)).

(a)

Let $y = 0$, $x = e_x$, and $\omega t = 0$; solving for the stiffness and damping coefficients gives

$$K_x e_x(1) - B_x e_x \omega(0) = \left(F_0\right)_x \cos(0 + \varphi_x)$$

$$K_x = \frac{\left(F_0\right)_x \cos \varphi_x}{e_x} \qquad \text{(A7)}$$

$$K_y e_y(0) + B_y e_y \omega(1) = \left(F_0\right)_y \sin(0 + \varphi_y)$$

$$B_y = \frac{\left(F_0\right)_y \sin \varphi_y}{e_y \omega} \qquad \text{(A8)}$$

Let $X = 0$, $y = e_y$, and $\omega t = \pi/2$; again solving for the stiffness and damping coefficients gives

$$K_x e_x(0) - B_x e_x \omega(1) = \left(F_0\right)_x \cos\left(\frac{\pi}{2} + \varphi_x\right)$$

$$B_x = \frac{\left(F_0\right)_x \sin \varphi_x}{e_x \omega} \qquad \text{(A9)}$$

39

$$K(e_y)(1) + Be_y \omega(0) = \left(F_0\right)_y \cos \varphi_y$$

$$K_y = \frac{\left(F_0\right)_y \cos \varphi_y}{e_y} \tag{A10}$$

The transmitted forces in the X-Y plane are measured along with the journal displacements in orthogonal planes. The rotor frequency ω is also measured. When these values are known, the dynamic film coefficients in the X-Y planes can be solved for.

REFERENCES

1. Vance, John M.; and Royal, Allen C.: High Speed Rotor Dynamics - An Assessment of Current Technology for Small Turboshaft Engines. J. Aircr., vol. 12, no. 4, Apr. 1975, pp. 295-305.

2. Hamburg, Glenn W.; et al.: Design and Development of Low-Cost, Self-Contained Bearing Lubrication Systems for Turbine Engines. J. Aircr., vol. 12, no. 4, Apr. 1975, pp. 253-259.

3. Tessarzik, J. M.; Badgley, R. H.; and Anderson, W. J.: Flexible Rotor Balancing by the Exact Point-Speed Influence Coefficient Method. J. Eng. Ind., vol. 94, no. 1, Feb. 1972, pp. 148-158.

4. Den Hartog, Jacob P.: Mechanical Vibrations. Fourth Edition, McGraw-Hill Book Co., Inc., 1956, pp. 210-211.

5. Hagg, A. C.; and Sankey, G. O.: Oil Film Properties with Reference to Unbalance Vibration. J. Appl. Mech., vol. 23, no. 2, June 1956, pp. 302-306.

6. Brown, P. F.: Bearings and Dampers for Advanced Jet Engines. SAE paper 700318, Apr. 1970.

7. Trivisonno, Roger J.: Fortran IV Computer Program for Calculating Critical Speeds of Rotating Shafts. NASA TN D-7385, 1973.

8. Lund, J. W.: Rotor Bearing Dynamics Design Technology, Part V: Computer Program Manual for Rotor Response and Stability. AFAPL-TR-65-45, Mech. Tech. Inc., 1965. (Available from DDC as AD-470315.)

9. Mohan, S.; and Hahn, E. J.: Design of Squeeze Film Damper Supports for Rigid Rotors. J. Eng. Ind., vol. 96, no. 3, Aug. 1974, pp. 976-982.

10. Barrett, L. E.; and Gunter, E. J.: Steady State and Transient Analysis of a Squeeze Film Damper Bearing for Rotor Stability. NASA CR-2548, 1975.

11. Cunningham, Robert E.; Fleming, David P.; and Gunter, Edgar J. Jr.: Design of a Squeeze-Film Damper for a Multi-Mass Flexible Rotor. J. Eng. Ind., vol. 97, no. 4, Nov. 1975, pp. 1383-1389.

12. Dimentberg, F. M.: Flexural Vibrations of Rotating Shafts. Butterworths (London), 1961, p. 191.

13. Tonnesen, J.: Experimental Parametric Study of a Squeeze Film Bearing. J. Lubr. Technol., vol. 98, no. 2, 1976, pp. 206-213.

14. White, D. C.: The Dynamics of a Rigid Rotor Supported on Squeeze Film Bearings. Conference on Vibrations in Rotating Systems, Inst. Mech. Eng. (London), 1972, pp. 213-229.

15. Simandiri, S.; and Hahn, E. J.: Effect of Pressurization on the Vibration Isolation Capability of Squeeze Film Bearings. J. Eng. Ind., vol. 98, no. 1, 1976, pp. 109-117.

1. Report No. NASA TP-1094	2. Government Accession No.	3. Recipient's Catalog No.
4. Title and Subtitle INFLUENCE OF OIL-SQUEEZE-FILM DAMPING ON STEADY-STATE RESPONSE OF FLEXIBLE ROTOR OPERATING TO SUPERCRITICAL SPEEDS		5. Report Date December 1977
		6. Performing Organization Code
7. Author(s) Robert E. Cunningham		8. Performing Organization Report No. E-9091
9. Performing Organization Name and Address National Aeronautics and Space Administration Lewis Research Center Cleveland, Ohio 44135		10. Work Unit No. 505-04
		11. Contract or Grant No.
12. Sponsoring Agency Name and Address National Aeronautics and Space Administration Washington, D.C. 20546		13. Type of Report and Period Covered Technical Paper
		14. Sponsoring Agency Code

15. Supplementary Notes

16. Abstract

Experimental data were obtained for the unbalance response of a flexible rotor to speeds above the third lateral bending critical. Squeeze-film damping coefficients calculated from measured data showed good agreement with short-journal-bearing approximations over a frequency range from 5000 to 31 000 cpm. Response of a rotor to varying amounts of unbalance was investigated. A very lightly damped rotor was compared with one where oil-squeeze dampers were applied.

17. Key Words (Suggested by Author(s)) Unbalance response; Vibrations; Viscous damping; Flexible rotor; Supercritical	18. Distribution Statement Unclassified - unlimited STAR Category 07		
19. Security Classif. (of this report) Unclassified	20. Security Classif. (of this page) Unclassified	21. No. of Pages 43	22. Price* A03

1   1 1U,A,   113077 S00903DS
DEPT OF THE AIR FORCE
AF WEAPONS LABORATORY
ATTN: TECHNICAL LIBRARY (SUL)
KIRTLAND AFB NM 87117

NASA